Insight into the inclusion of heteroatom impurities in Silicon structures

Rita Maji*

Dipartimento di Scienze e Metodi dell'Ingegneria,
Università di Modena e Reggio Emilia,
Via Amendola 2 Padiglione Tamburini , I-42122 Reggio Emilia, Italy

Eleonora Luppi

Laboratoire de Chimie Théorique, Sorbonne Université and CNRS F-75005 Paris, France

Elena Degoli†

Dipartimento di Scienze e Metodi dell'Ingegneria,
Università di Modena e Reggio Emilia and Centro Interdipartimentale En&Tech,
Via Amendola 2 Padiglione Morselli, I-42122 Reggio Emilia, Italy
Centro S3, Istituto Nanoscienze-Consiglio Nazionale delle Ricerche (CNR-NANO),
Via Campi 213/A, 41125 Modena, Italy
Centro Interdipartimentale di Ricerca e per i Servizi nel settore della produzione,
stoccaggio ed utilizzo dell'Idrogeno H2–MO.RE.,
Via Università 4, 41121 Modena, Italy

Julia Contreras-García‡

Laboratoire de Chimie Théorique, Sorbonne Université and CNRS F-75005 Paris, France

arXiv:2205.14468v1 [cond-mat.mtrl-sci] 28 May 2022

(Dated: May 31, 2022)

Abstract

The bonding properties of tilt boundary in poly-silicon and the effect of interstitial impurities are investigated by first-principles. In order to obtain thorough information on the nature of chemical bondings in these solid systems, an accurate topological analysis is performed, through partitioning of the electron localization function. Although the mechanism of segregation of single light impurities, such as carbon, nitrogen and oxygen in Si-based systems is known, it is only in the presence of multiple segregation that the distinctive structures of the various interstitial impurities emerge. The structural analysis of the modified Si systems and the comparison with the corresponding molecular structure within these solid phases provide an adequate description of interesting properties, for which bond charges provides more insight than bond length. It is shown that, in the presence of isovalent carbon, all systems try to preserve the tetrahedral coordination, on the contrary, trivalent nitrogen induces a strong local distortion to fit in the tetrahedral Si matrix while oxygen is the impurity that segregates more easily and more regularly. This work shows that impurities lead to local distortions and how the electron distribution rearranges to smooth it. Overall, it shows how the analysis of bonds and their correlation with energetics and electronic structure is of fundamental importance for the understanding of the defects induced properties and of the basic mechanisms that influence them.

[*] rita.maji@unimore.it

[†] elena.degoli@unimore.it

[‡] contrera@lct.jussieu.fr

I. INTRODUCTION

The existence of defects is inherent in materials, despite the more and more efficient growth techniques. [1] Defects may cost energy to be created, however, in some cases the configurational entropy can make favorable the incorporation of a certain concentration of defects in order to lower the free energy of the system. [2] Moreover, impurities are also often intentionally introduced to modify material properties, such as doping of semiconductors with acceptors and donors is essential for electronic and optoelectronic applications. [3–5]

In silicon-based devices, defects such as impurities, vacancies, interstitial and grain boundaries (GBs) modify the functionality and the performance of the devices. [1, 6–8] In this context, polycrystalline silicon (poly-Si) is very attractive for several technological applications [8, 9]. However, its efficiency can be strongly modified because poly-Si is characterized by a high density of GBs which are the primary hindrance to its functionality. Furthermore, the electrical properties of poly-Si and GBs are additionally altered by the complex interaction with intrinsic point defects (vacancies and/or self-interstitials) and/or impurity atoms, such as carbon, oxygen, nitrogen, and various types of metals. [7, 10, 11] Moreover, the interaction of these light impurities (C, O, N) with poly-Si under certain circumstances can facilitate the formation of microstructures of SiC, SiO_2, and Si_3N_4[10].

Oxygen defects in Si have been reported focusing on several aspects, such as doping concentration, different complexes, modification of electronic and mechanical properties. [12, 13] Carbon defects studies focused on self-interstitial trapping mechanism[14], C-C complexes[15], and transient enhanced diffusion of other impurities[14]. Nitrogen defects have been considered as one of the key dopants for exceptional enhancement of mechanical stability[16, 17]. Moreover, recently electronic and optical properties in crystalline Si hyperdoped with N is reported as a source of sub-bandgap absorptance[18].

Most of the previous first-principles works focused on the understanding of the complex mechanisms in polycristalline Si following experimental observations. Even if this characterization provides information about the local performance of such areas, a correlation to the light impurity distribution remains ambiguous.

Another approach, increasingly popular for crystalline systems in the past decade, is the analysis of the chemical bonding based on the topological analysis obtained from density distribution. In particular, electron localization function (ELF) [19–21] has emerged as a

powerful tool to understand the behavior of the electrons in atoms, molecules and solids. A great variety of bonding situations can be explained and therefore interpreted in relation to physical properties. [21–28]

In this work, we highlight on chemical bonding of the C, N and O local structures in Silicon bulk and in Silicon GB $\Sigma3\{111\}$ with and without vacancies. In order to understand the organization and the underlying electronic structure of the inclusion of C, O and N atoms in Si structures, we focus on topological analysis obtained from density distribution. We present the characteristics of electron localization function (ELF) obtained from first-principles calculations. [19–21] ELF analysis contribute to the understanding of the behavior and properties of C, N and O atoms in Silicon structures by the characterization of the chemical bonding.

II. METHODOLOGY

A. Systems

The $\Sigma3\{111\}$ Si GB consists of two Si grains, misoriented by an angle $\Omega = 60°$ which form an interface along the crystallographic plane $\{111\}$ (coincidence site lattice). To describe the grain, we used an orthorhombic supercell ($a \neq b \neq c$ and $\alpha = \beta = \gamma = 90°$) composed of 96 Si atoms generated with *GB Studio program*. [29]. The lattice parameters are a=13.30 Å, b=7.68 Å and c=18.81 Å. [8] The formation energy of the $\Sigma3\{111\}$ Si GB is $E^{\mathrm{f}}_{\mathrm{GB}} = 0.002$ eV/Å^2 ($E^{\mathrm{f}}_{\mathrm{GB}} = 0.05$ J/m^2) [8] which indicates that this GB has a very regular structure, i.e. bond lengths and angles are close to bulk silicon. [30, 31] This is also the most stable GB since there are no dangling bonds and little bond distortions. [8, 32]

We consider the structure of Si bulk as the reference to compare our results. In this case, we used a cubic supercell ($a = b = c$ and $\alpha = \beta = \gamma = 90°$) of 64 atoms with a=10.86 Å. This value for a was deduced from the experimental lattice constant 5.431Å, for a face-centered cubic unit cell of two Si atoms. [33].

Then, we create a vacancy in the $\Sigma3\{111\}$ Si GB. There exists only two distinct positions of Si where vacancies can be created. [8] These vacancies are indicated throughout the paper as V1 and V2 and are shown respectively in panels (b) and (c) of Fig. 1. The formation energy of the vacancy V1 in the GB is $E^{\mathrm{f}}_{\mathrm{VGB}} = 2.91$ eV while for the vacancy V2

we found $E^{\mathrm{f}}_{\mathrm{VGB}} = 3.04$ eV. [8] The presence of the vacancy induces coordination defects. Most specifically, both in V1 and V2 we have two Si atoms that are threefold coordinated while all the other Si atoms are fourfold coordinated.[8] These atoms are easily identified in Fig. 1 as those having a lone pair (brown sphere).

To study the role of C, N and O impurities, we have sequentially inserted from one to four of these atoms as interstitials in Si-bulk and in the Si GB with and without vacancies. Different configurations were found but only lowest total energy ones are reported in each case. More details can be found in Ref.[7].

B. Computational method

1. *Energetics*

The calculations were performed using density functional theory (DFT) as implemented in the plane-wave based Vienna Ab initio Simulation Package (VASP)[34, 35] We employed the generalised gradient approximation PBE (Perdew–Burke–Ernzerhof) for the exchange-correlation functional [36] and projector augmented-wave (PAW) pseudopotentials with a cutoff of 400 eV. K-points sampling within the Monkhorst Pack scheme [37] was used for integration of Brillouin-zone together with the linear tetrahedron method including Blöchl corrections. [38] We used a k-mesh of 3×3×3. For the structural optimisation, we used a force threshold value of 10^{-2} eV/Å per atom. For all the systems the total energy is calculated as the total energy of the unit cell where all the atoms are interacting. Moreover, the pressure of the systems is calculated directly from VASP and it is the hydrostatic pressure of a cell of a given volume. Finally, in these calculations we did not include the spin polarization. [18, 39]

Formation energy ($E^{\mathrm{XB}}_{\mathrm{f}}$) in bulk Si is calculated as

$$E^{\mathrm{f}}_{\mathrm{XB}} = E_{n_{\mathrm{X}}+\mathrm{B}} - E_{\mathrm{B}} - n_{\mathrm{X}}\mu_{\mathrm{X}}. \quad (1)$$

Here X: C/N/O refer to different impurity elements, $E_{n_{\mathrm{X}}+\mathrm{B}}$ and E_{B} are the total energies of Si bulk containing n_{X} number of impurity atoms and of pristine Si bulk, respectively. μ_{X} is the chemical potential of impurity elements (X: O/N/C), calculated as the energy per atom of an O_2 molecule in vacuum for oxygen, as the energy per atom of an N_2 molecule in

vacuum for nitrogen and for C, it is calculated from diamond phase.

Formation energy ($E_{\mathrm{f}}^{\mathrm{XGB}}$) in Si GB is calculated as

$$E_{\mathrm{XGB}}^{\mathrm{f}} = E_{n_{\mathrm{X}}+\mathrm{GB}} - E_{\mathrm{GB}} - n_{\mathrm{X}}\mu_{\mathrm{X}}, \tag{2}$$

where $E_{n_{\mathrm{X}}+\mathrm{GB}}$ and E_{GB} are the total energies of Si GB containing n_{X} number of impurity atoms and of pristine Si GB, respectively.

Formation energy ($E_{\mathrm{f}}^{\mathrm{XVGB}}$) in Si GB with vacancy is calculated as

$$E_{\mathrm{XVGB}}^{\mathrm{f}} = E_{n_{\mathrm{X}}+\mathrm{VGB}} - E_{\mathrm{VGB}} - n_{\mathrm{X}}\mu_{\mathrm{X}} \tag{3}$$

$E_{n_{\mathrm{X}}+\mathrm{VGB}}$ is the total energies of Si GB containing n_{X} number of impurity atoms in presence of a vacancy and E_{VGB} is the energy of Si GB with a vacancy. [7]

2. *Chemical bond*

To study the structural changes induced by the impurities in the Si-bulk, and in the Si GB with and without vacancies we have analysed bond lengths and the bond charges [40].

In order to dissect bond charges we have resorted to the Electron Localization Function (ELF). Becke and Edgecombe [41] introduced the ELF as a local measure of electron localization. Its core, χ, reflects the Pauli principle as a local measure of electron kinetic energy density. More specifically, it depends on the Pauli kinetic energy density, t_P (where the bosonic contribution has been taken away), renormalized by the kinetic energy density in the homogeneous electron gas, t_{TF}:

$$\chi = \frac{t_P}{t_{TF}}. \tag{4}$$

It is desirable to delimit electron localization and to obtain a direct relationship between the localization and the function. For those reasons, it was mapped following the lorentzian function $\eta = \frac{1}{1+\chi^2}$, so that when η tends to 1 electrons are highly localized, whereas η tends to 0.5 in those regions where the electrons follow the homogeneous electron gas distribution (i.e. delocalized).

Following Bader's approach [42], this function can be analyzed within the dynamical

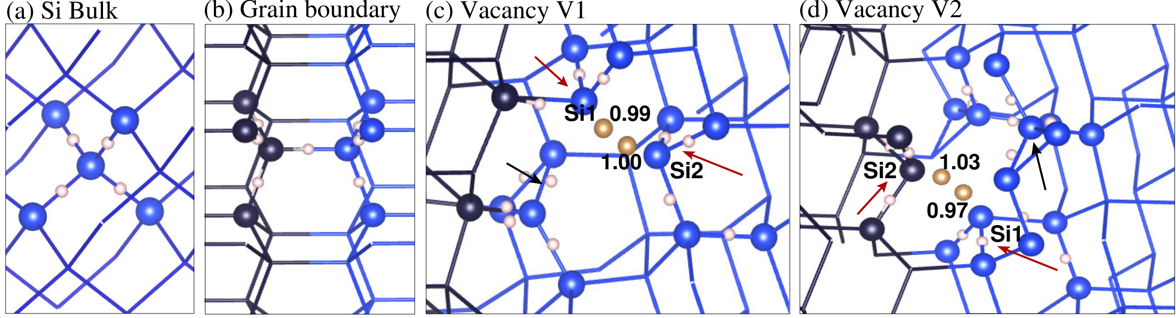

Figure 1. Structures of a) Si bulk b) Grain boundary (GB) and vacancy sites c) V1 d) V2. Silicon atoms in blue. Bonds and lone pairs are highlighted with small white and brown spheres respectively. Amplitude for lone pairs have been mentioned, 3-fold coordinated sites in (c, d) marked as Si1 and Si2. Light and dark blue have been used in order to highlight the grain boundary. Only Si atoms, for which connected bonds are shown here, are represented with "balls". Triangular and pyramidal conformation marked with black and red arrows respectively.

system theory context [43] to induce a partition into non overlapping basins. The gradient of the ELF is the key function to recover chemical entities in real space. In general, the ELF presents a variable topology with mountains, valleys, plateau zones, and different kinds of critical points (maxima, saddle, ring, and cage points) where the ELF gradient vanishes. Zero flux surfaces of the ELF gradient enclose 3D regions or basins that can be associated with electron shells and sub-shells, bonds, and lone pairs. The power of the ELF partition in the case of crystalline systems lies in the fact that these basins are finite, disjoint, and space filling, which means that adding all of them up, we recover the macroscopic volume. Integration of the electron density within those basins leads to bond and lone pair charges that also recover the total number of electrons when added together.

We have resorted to the `CRITIC` code [44] in order to compute basin charges (q). In all cases, we have checked the performance of the partition by adding up all the volumes of the basins in which the unit cell is split, since the total unit cell volume should be recovered.

III. RESULTS

A. Pure silicon

Results for pure silicon are shown in Fig. 1(a). Bulk silicon has a regular tetrahedral coordination with a Si-Si covalent bond (ELF maxima shown as white spheres) holding 2 electrons. When the grain boundary is introduced (Fig. 1b) the bonding is very much

preserved in the four-folded atoms: we observe the appearance of an elongated Si-Si bond (2.37 Å) with a slightly smaller charge (1.98 electrons) that joins the two domains (different colors have been used in order to highlight the grain boundary).

The introduction of vacancies leads to important bonding changes (Fig. 1c-d). 3-fold coordinated Si atoms appear which lead in both V1 and V2 to an overall increase of the charge in the neighboring Si-Si bonds (2.01-2.07e). The 3-folded atoms appear in most cases in a pyramidal structure, with a lone pair on each Si taking the direction of the "missing" Silicon atom. These lone pairs (in brown) hold roughly 1 electron each (0.99-1.0 electrons) in V1. A greater charge asymmetry is found in V2, where lone pairs hold 1.03 and 0.975 electrons each. Note that in both cases, the two lone pairs add up to the 2 electrons expected for the missing Silicon bond. On top of the pyramidal conformations, a planar triangular conformation is also observed in V1 where instead of the lone pairs, two confronted Si atoms form a new bond with two ELF maxima. This new bond (highlighted with an arrow in Fig. 1c, 1d), although weaker than the others (1.54 electrons) allows the atoms involved to recover the 4-fold coordination.

Finally, it is worth noting that in non-strained cases, as is the case of the grain boundary bond in Fig. 1b, the bond appears on the internuclear line. Instead, strained bonds are characterized by ELF maxima outside of the bonding line. This is the case of both V1 and V2, where many of the bonds of the 3-folded atoms are offset. Note that hydrostatic pressure of Si bulk super cell and Si GB are respectively 1.973 GPa and 1.89 GPa. Whereas in presence of vacancy (V1, V2) hydrostatic pressure of Si GB is P(V1GB)=1.42 GPa and P(V2GB)=1.402 GPa, respectively.[8] The different pressure in the vacancies can be understood from the position of the vacancies with respect to the grain boundary: whereas V1 lies within one of the domains, V2 lies at the border. This will lead (see below) to important differences when impurities will be adsorbed.

B. Carbon

Given the stable Si bulk and GB structures, it is unfavorable to introduce an extra C atom (see Formation energy in Fig. 16, discussed later). The C atom is 3-fold coordinated in both cases, and places the rest of its valence charge in lone pairs (Figs. 2a-b): two lone pairs in bulk Si with 0.13+0.012=0.142 electrons in total and one lone pair in the GB

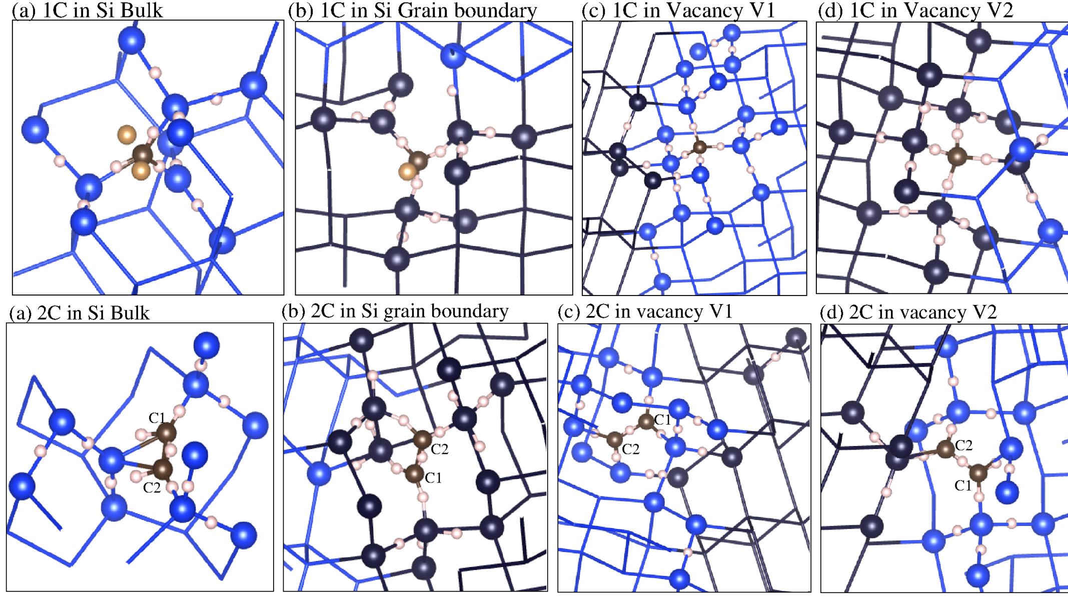

Figure 2. Structures with the inclusion of 1 (top) and 2 (bottom) carbon atom(s) in a) bulk Si b) GB b) V1 c) V2. Silicon atoms in blue and carbon atoms in dark brown. Bonds and lone pairs are highlighted with small white and brown spheres respectively.

with 0.6 electrons. Very low population lone pairs are usually only observed in delocalized and/or unstable configurations. Another signature of instability are the strained C-Si bonds shown both in bulk (see SI: Table XIII in comparison to bulk SiC value of Table I) and GB (see SI: Table XIV in comparison to bulk SiC value of Table I). The image in the case of vacancies, where there is space for the inclusion of the atom, is very different (Figs. 2c-d). Carbon belonging to the same group as Si, it is able to take up Si missing positions in the case of vacancies. This is what we observe in the case of V1 and V2: symmetric tetrahedral arrangements are obtained around carbon. Moreover, C and Si have similar electronegativities, leading to 2 electron bonds (see SI: Table XV, XVI). Note that in the case of V1 bonds are strained, whereas they are not in V2 (i.e. bond charges are offset). Noteworthy, V1 leads to a greater bond length scattering (1.99-2.03 Å) than V2 (2.01-2.03Å).

Fig. 3 shows Si-Si and Si-C bond charges and lengths in the different systems. The red line provides the bulk Si reference value, while the blue line provides the bulk SiC reference value. We can see that charges (Fig. 3 top) shed more light on the electronic structure of these strained systems than distances (Fig. 3 bottom). Indeed, both Si-Si and Si-C distances are spread around the reference values indicating a strained structure. Instead, bond charges in the V1 and V2 systems are very close to the nominal values of the two (whereas distances

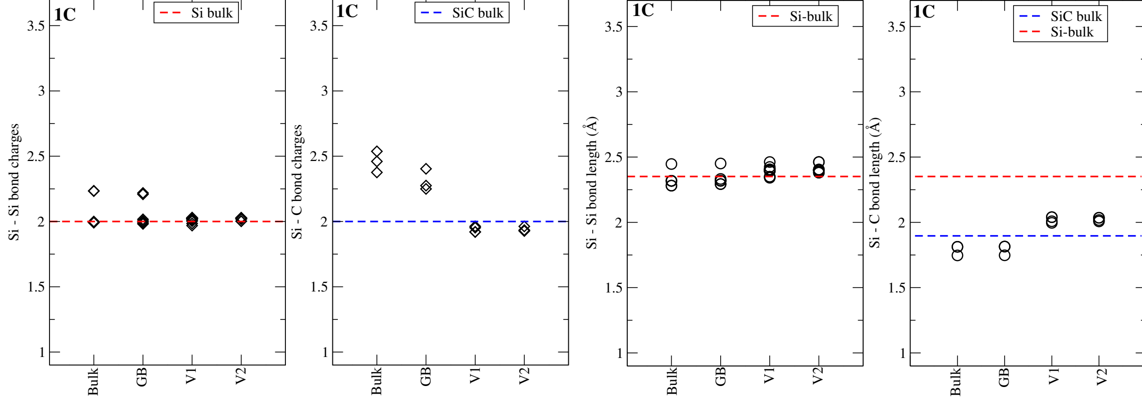

Figure 3. Bond charge and bond length variation of Si-Si and Si-C bonds for the inclusion of one carbon atom in Si-bulk, Si-GB and in presence of vacancy V1 and V2. As a reference Si-Si/Si-C bond charges/lengths from cubic bulk phases of Si and SiC are marked by dotted lines in respective plots.

are not). In other words, the vacancy systems are able to relax to lead to a stable electronic conformation, even if the structure is locally distorted. We will thus in the following mainly focus on the charges.

As we have seen, bulk and GB systems with 1C impurity are not able to easily accommodate the carbon atom and lead to offset bond charges, and even to lone pairs. In general, a charge flow towards the impurity is observed in bulk and GB, with greater Si-Si and Si-C charges than in the undoped case.

When two carbon atoms are introduced in the silicon systems (Fig. 2 bottom), the two C atoms are always found forming a C-C bond in an arrangement similar to ethylene: two Si atoms are attached to each C (i.e. 3-fold coordinated). Among the four systems, a slight difference appears in the coordination in the case of bulk silicon. The little place available in the case of the bulk leads to a Si atom coordinated to the C=C unit in a similar fashion to the Dewar–Chatt–Duncanson model. The charge involved in each of these C-Si bonds is of 1.76 e. In the case of GB, a unit rather close to ethylene is found, with a C-C charge slightly lower than in C_2H_2 (ELF calculation on molecular ethylene leads to a C-C bond charge of 3.4 e - blue line in Fig. 4). In the case of the vacancy systems, and in spite of the 3-fold coordinated C atoms, the C-C bond holds 2.3 e, much closer to that of ethane than ethylene. Overall, a charge deficiency is observed in the C-C bond, which is balanced by a higher charge in the C-Si bonds of ca. 2.4 e. Exceptions are the coordination Si-C bonds in the bulk and some of the bonds in the GB. The charge balance thus happens locally, so

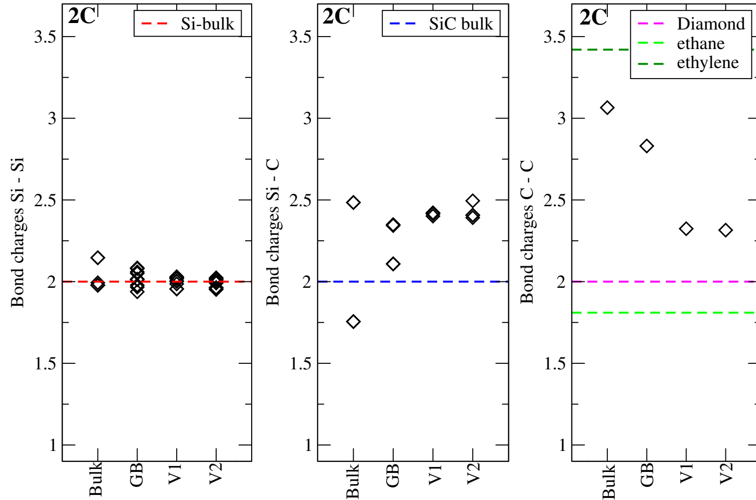

Figure 4. Bond charge variation of Si-Si, Si-C, and C-C bonds for the inclusion of two carbon atoms in Si-bulk, Si-GB and in presence of vacancy V1 and V2. As a reference, Si-Si/Si-C bond charges from cubic bulk phases of Si and SiC, and C-C bond charges from diamond, ethane and ethylene are marked as mentioned in the inset of respective plots.

that a little Si-Si bond charge dispersion is found (Fig. 4).

Three carbon atoms (Fig. 5 top) show different patterns depending on the Si structure. Bulk and vacancies lead to the formation of a triangular structure, whereas in the grain

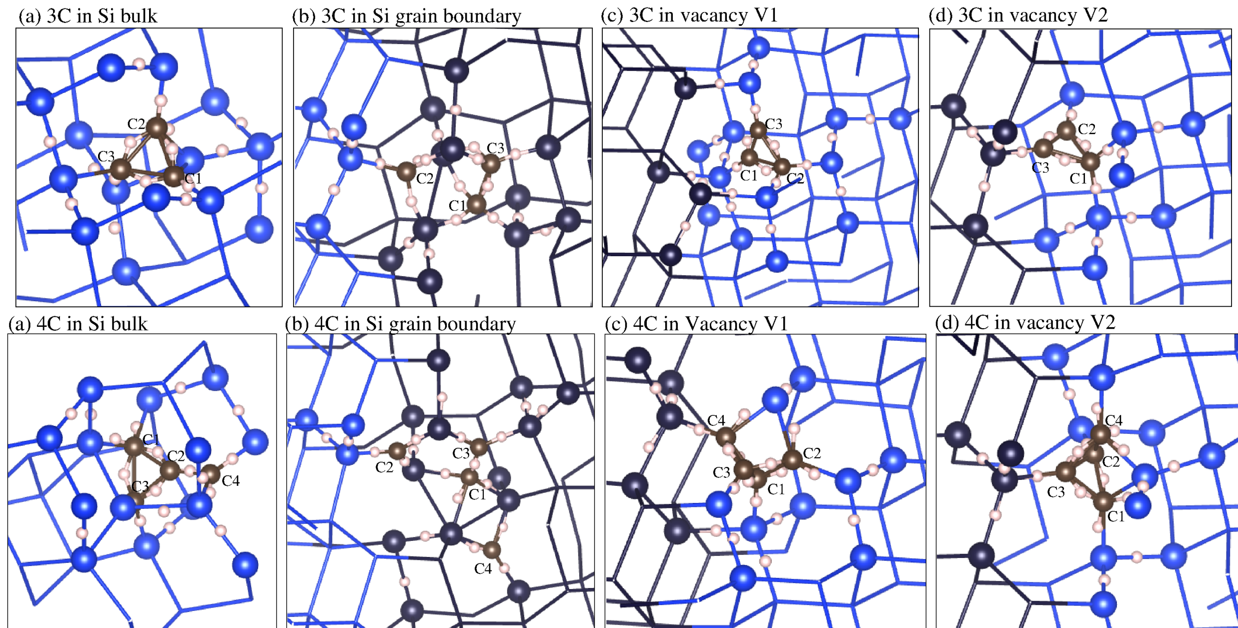

Figure 5. Structures with the inclusion of three (top) and four (bottom) carbon atoms in a) bulk Si b) GB b) V1 c) V2. Silicon atoms in blue. Bond charges are highlighted with small white spheres. Lone pairs with values ≤ 0.01 not shown here are mentioned in SI: Table XIII, XIV, XV.

boundary the 3C atoms are distributed separately.

A difference similar to the 2C inclusion appears between the bulk and the vacancies: a coordinated Si bridge appears in the bulk. In this case, the bridge in the bulk leads to all the 3C atoms being four fold coordinated with all C having 2 C-C bonds and 2 Si-C bonds. C-C bonds hold 1.5-1.6 e. C-C bonds are hence close to the single bonds in cyclopropane (1.7 e). The C-Si bridge shows the same pattern as for the 2C atoms: Si-C populations are high (2.4 e) for the terminal bonds and lower (1.9 e) for the bridge bonds.

Instead, in the vacancies two carbon atoms are 3-fold coordinated, leading to a unit similar to cyclopropene: they show two single 1.5 e bonds and one double 3.0 e bond (Fig. 6). This is to be compared with cyclopropene which has 1.8 e in the C-C bond and 3.2 e in the C=C one.

Just like in molecular cycles in general, bonds are very strained, which is reflected in the electron pair localized outside of the C-C bonding line. Note that a smaller strain is found in V2 than in V1 (maxima are closer to the internuclear lines), which explains the easier formation of the inclusion of 3C in V2 than in V1 (0.9758 eV and 0.8144 eV in V1 and V2, respectively - see SI: Table IV).

Si-C bonds next to the bridge in the bulk and next to the double bond in the vacancies are highly populated, releasing again the charge from the "strained" areas. This leads again to Si-Si bonds close to 2 e except for slight deviations close to the bridging Si atom.

If we now look at the organization in the grain boundary we see that the 3C atoms are distributed separately: one C-C bond inside a domain and one separate C atom at the boundary. The separate C atom, just like for the 1C inclusion, shows a small lone pair (LP) with negligible charge. In this case, the C-C bond corresponds to an ethane configuration, with both carbon atoms being four folded. The C-C bond charge is consequently smaller than in the 2C case, with only 1.57 e. The Si-C charges are very variable. This is again linked to the appearance of a bridge atom, where the Si-C charge is 1.5e, whereas the terminal C-Si bonds hold 2.1-2.2e. This also leads to the appearance of a higher Si-Si bond charge (2.2 e) at the β bridge position (bond next to the Si-C bridge).

Four carbon atoms (Fig. 5 bottom) are difficult to intercalate all together, so they lead to very different conformations in the various matrices. In the bulk they adopt a methylenecyclopropane arrangement. The methylene bond holds 3 e. The bonds within the cyclopropane hold ca. 2 e, except for the bond opposite to the methylene, which holds 1

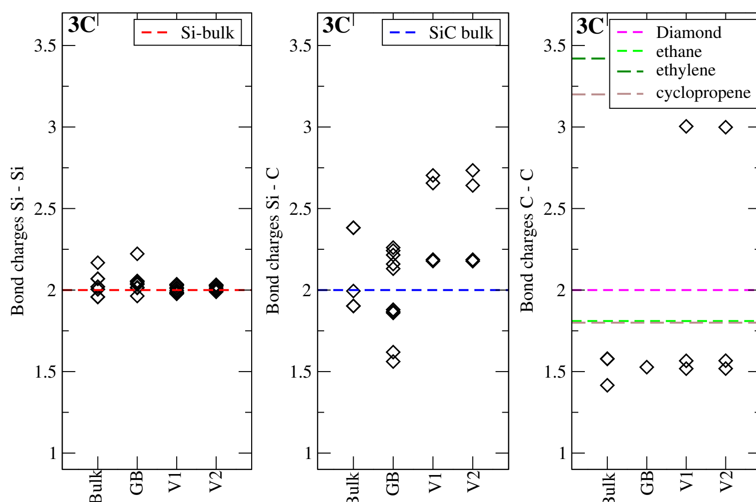

Figure 6. Bond charge variation of Si-Si, Si-C, and C-C bonds for the inclusion of three carbon atoms in Si-bulk, Si-GB and in presence of vacancy V1 and V2. As a reference, Si-Si/Si-C bond charges from cubic bulk phases of Si and SiC, and C-C bond charges from diamond, ethane, ehtylene and cyclopropene are marked in the inset of respective plots.

electron only. This weak bond is accompanied by the appearance of a small lone pair (0.02 electron) on one of its atoms. Overall this represents a rather unstable doping. The C-Si bonds show a charge of 1.8-1.86 e and the Si-Si bonds are in most cases nominal (2.0 e) except one β-Si-Si bond with respect to the C atoms holding the lone pair. This shows how this atom perturbs the structure in a longer range and highlights a general pattern in the bulk adsorption and the formation of bridges.

When a grain boundary exists, defaults and voids are present allowing separate carbon conformations: a C-C bond and two independent C atoms are adsorbed, all of them with uncommon coordinations: the independent atoms are 3-fold coordinated (C-Si bonds with 2.5 e in one of the atoms and 2.1-2.7 for the other one). The C-C bond also shows one of its ends with a 3-fold coordination and a C-C bond of 2.5 electrons. The different coordinations are balanced out to a good extent by the populations. Whereas the 4-folded carbon has two deficient bonds (C1: 1.1. and 1.7), the 3-folded atom has two overpopulated C-Si bonds (C3: 2.2 and 2.3) (SI: Table XIV). The Si structure shows in general little perturbations except again for the Si-Si bond β with respect to the 3-folded atom in the C-C bond.

In the presence of vacancies, the bicyclobutane is the most stable organization for both V1 and V2. The C atoms form a bicycle where a weak C-C bond is observed in the bridge (1.6 e and 1.36 e in V1 and V2, respectively). The other C-C bonds are single and strained

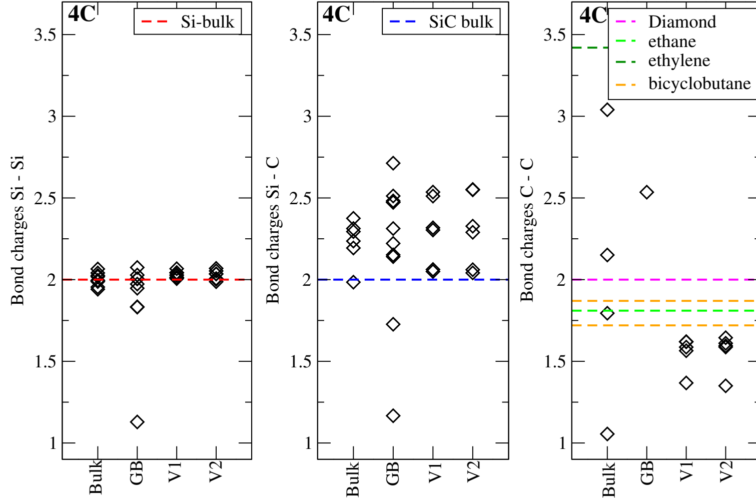

Figure 7. Bond charge variation of Si-Si, Si-C, and C-C bonds for the inclusion of four carbon atoms in Si-bulk, Si-GB and in presence of vacancy V1 and V2. As a reference, Si-Si/Si-C bond charges from cubic bulk phases of Si and SiC, and C-C bond charges from diamond, ethane, ethylene and bicyclobutane are marked in the inset of respective plots

(1.55-1.6 e). The head C-Si bonds are again strained due to the tension induced by the bicycle. This leads to smaller charges (2e) with respect to the other C-Si bonds (2.3 for the head C-Si bonds, even 2.0 in V1, and 2.5 for the bridge atoms). Although unstable, the bicycle structures lead to only local perturbations, with Si-Si bonds holding charges very close to the nominal 2.0 electrons. This is easily seen in Fig. 7 top left, where the dispersion in V1 and V2 of Si-Si values is very small. Note that once again, this does not correspond to the Si-Si distances image (see SI: Fig.28), where for example in V1 a greater distance is observed. Nevertheless, the structure rearrangement manages to preserve the Lewis structure. Note that the formation energy of these structures (SI: Table IV) is given by 2.2861 eV and 2.1306 eV for V1 and V2, respectively. Once again, the local distortion of V2 requires a slightly smaller energy than V1.

Fig. 8 summarizes the trends with the number of atoms. We can see that the Si matrix is more affected in the bulk and GB structures than V1 and V2. In all cases, the charge dispersion increases as we increase the number of dopants, reflecting the difficulty to fit them into the matrix. One exception is the inclusion of 4C in V1 and V2, which leads to a smaller dispersion than 3C. Lone pair charges have also been included in blue. This allows to identify the cases in which charges cannot be accommodated in bonds. Looking at their respective charges, we can see that even in the case they appear, their charge is negligible

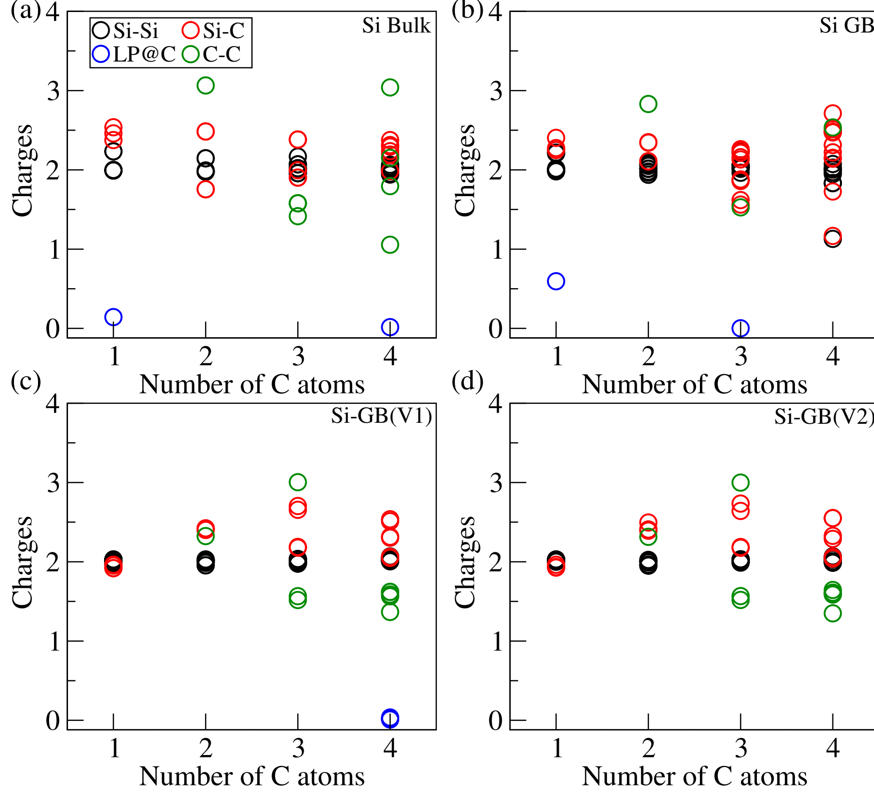

Figure 8. Bond charges (Si-Si, Si-C and C-C) and lone pairs at C (LP@C) variation for the inclusion of different numbers of carbon atoms in a)bulk Si b) GB c) V1 d) V2.

with one exception only, the lone pair for 1C in the GB. If we now check the general trends in formation energy (Fig. 16), we can see that bulk and GB on the one side and V1 and V2 on the other follow parallel trends with the only exception of 3C, where the separate inclusion of 2C and 1C in the GB seems more favorable than the 3 atoms together in the bulk.

C. Nitrogen

In this case it is worth starting by analyzing the stable Si-N mixture, Si_3N_4 (SI: Fig. 17). In this compound, where valences are naturally compensated, Si is 4-fold coordinated and N is 3-fold coordinated. The Si-N distance is 1.75Å and Si-N bond charge is 2.3 e. Each N atom holds two lone pairs of 0.528 e each (see SI: Table I). Taking into account the coordination, total charge leads to 7.96 e around the nitrogen atom.

When we introduce one N atom in the Si matrices, two different arrangements appear: 2-fold coordination with one LP, and 3-fold coordination with 2 LPs. The first case is observed

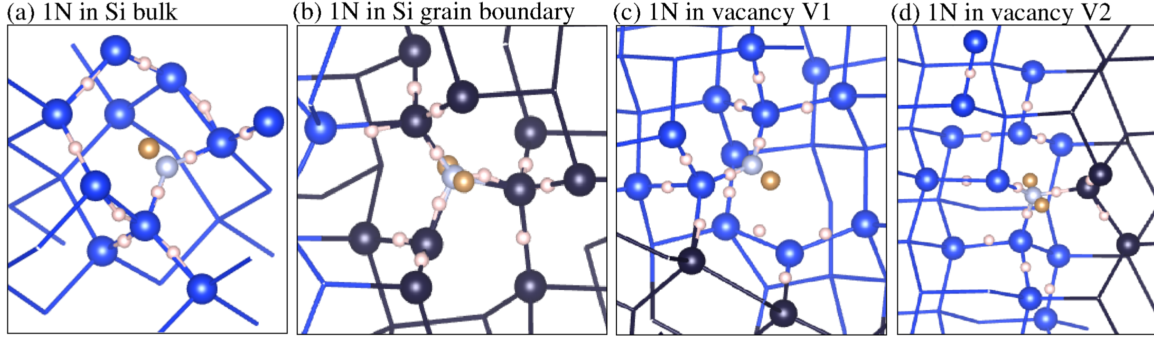

Figure 9. Structures with the inclusion of one nitrogen atom in a) bulk Si b) GB c) V1 d) V2. Silicon atoms in blue. Bonds and lone pairs are highlighted with small white spheres and brown spheres respectively.

in the bulk and in V1. In the bulk, the lone pair on N leads to a planar electronic symmetric distribution (ca. 2.4 e on each bond and on the LP). This structure leads to dispersion in the Si-Si bond charges, which show 1.9 e in the β bonds with respect to the inclusion. The configuration for the interstitial in V1 is similar to the one in the bulk: two fold coordinated and 1 LP. However, there is a bigger charge polarization. The LP holds 2.9 e and Si-N bonds have 1.7 e. A smaller charge Si-Si dispersion is observed in this case, with Si-Si bonds holding 1.95-2.0 e.

The GB enables N to be inserted in a 3-fold coordination. The bonds are lowly populated (1.75-2.0 e). Two LPs appear (1.9 e in total) to complete the Lewis structure. The arrangement for V2 is conceptually similar to the one in the GB for 1 Nitrogen atom: it is 3-folded with a slightly deficient population (1.95 e) and two LPs (1.69 e in total). However, a difference arises at the Si level: the 3-folded Si shows a LP (0.4 e) in the direction of the missing bond (SI: Table XX).

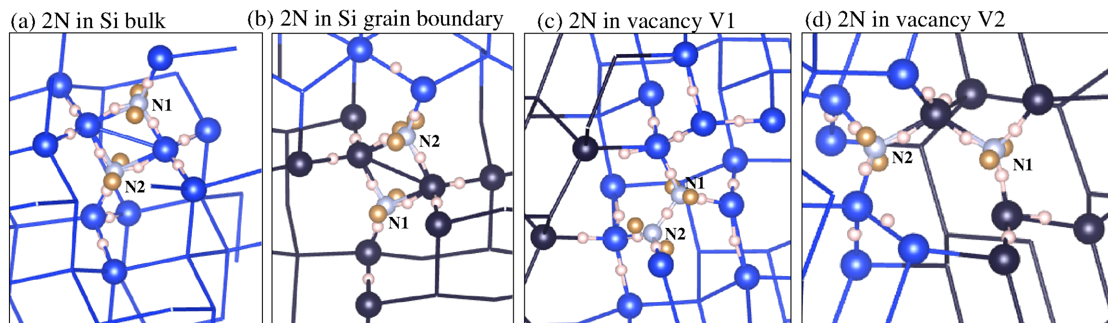

Figure 10. Structures with the inclusion of two nitrogen atoms in a) bulk Si b) GB c) V1 d) V2. Silicon atoms in blue. Bonds and lone pairs are highlighted with small white spheres and brown spheres respectively.

When we introduce 2N atoms in the bulk they alternate with Si atoms, instead of forming N-N bonds. This leads to a local configuration similar to Si_3N_4 (see SI: Table I): N is 3-fold coordinated and has 2 LPs. However, electrons are distributed differently: N-Si bonds hold 2-2.3 e and the lone pairs hold 0.7 e each. The total charge around N remains nevertheless similar, with 7.7 e. The GB leads to a similar structure, though N-Si bonds are slightly more populated (2-2.5 e). One of the N atoms remains with a similar LP distribution whereas in the other one, there is a LP split majorly in two (N2: 0.4 e + 0.5 e).

V1 is the only case we have observed where a N-N bond is formed (Fig. 10 c). This N-N bond is single, keeping the 3-fold coordination around each N. The N-N bond holds 1.45 e and each N shows two LPs whose added charge is in the range 2.8-3.1 e. V2 shows an structure similar to 1N, with the two N adsorbed around the same Si atom, lowly populated bonds (1.8-1.9 e) and two LPs (1.8 e in total). In all cases Si-Si bonds are overpopulated, even though a great dispersion of distances appears with Si-Si bonds both longer and shorter than in bulk Si (SI: Fig. 30).

The adsorption of three N atoms in bulk Si leads to two separate interstitials (Fig. 11a): a structure similar to 2N and an isolated N atom. This is similar to what was already observed for 3C in the bulk. The bond charges for the 2N complex are similar to the 2N results, though N LPs have smaller total charges (0.7-0.9 e). The remaining N atom is 3-fold coordinated by e-deficient bonds (1.8-1.9e) and shows 3 LPs which add up to 1.97 e. Bonds hold ca. 2 e except for the Si-N bonds which are not shared by the two nitrogen atoms, which hold ca. 2.3 e.

For V2 (Fig. 11d top), the adsorption takes place in a Si-N chain, with one of the terminal atoms only two-fold coordinated (aka N3). This atom shows highly populated Si-N bonds (2.5-2.7e) and two LPs which add up to 2.1 e. The N atom in the middle of the chain (aka N1) shows a high bond population in the direction of N3 (2.4e) and two LPs with a low charge of 1.25 e. The terminal 3-fold coordinated N atom (aka N2) has a 1.95 e bond with toward N1 and lowly populated bonds with the rest of the matrix (1.7-1.8 e). Its LPs add up to 2.1 e. We have thus different coordinations for the terminal atoms but both holding ca. 2 e in their LPs, whereas the intercalated N atom is surrounded by highly populated bonds, which leads to depleted LPs.

Both GB and V1 (Figs. 11b-c top) show a dendritic arrangement (all N atoms linked to the same Si atom). The globularity in the GB interstice is rather symmetric, with Si-N

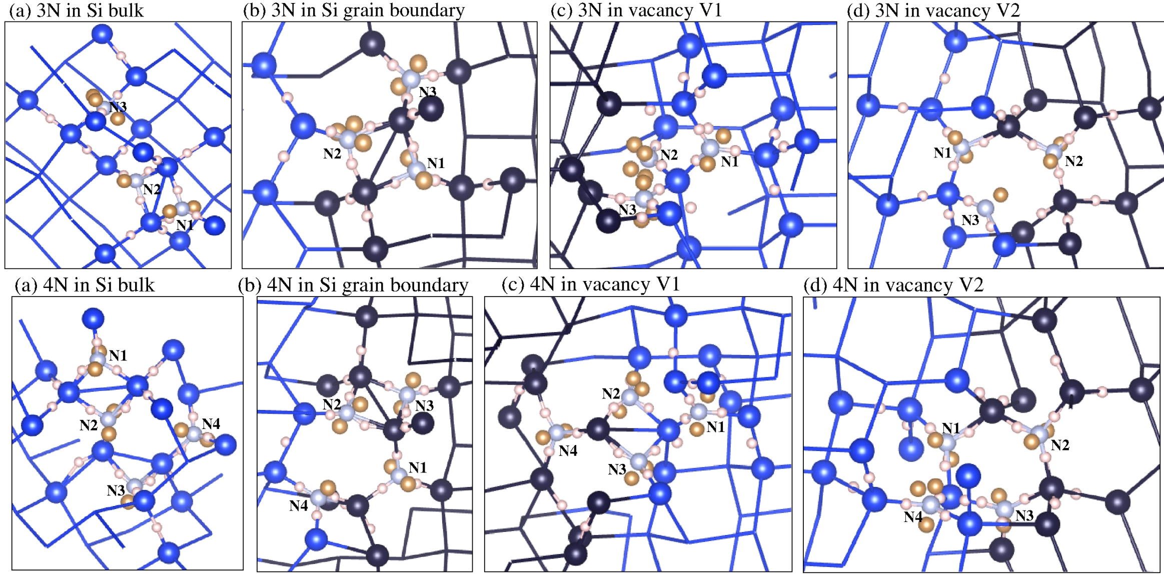

Figure 11. Structures with the inclusion of three (top) and four (bottom) nitrogen atoms in a) bulk Si b) GB c) V1 d) V2. Silicon atoms in blue. Bonds and lone pairs are highlighted with small white spheres and brown spheres respectively

bonds holding 1.7-1.8 e and LPs 1.1-1.2 e. V1 structure shows instead a bigger asymmetry since one of the N atoms (aka N2) is only 2-fold coordinated. This atom has Si-N bonds of ca. 2.3 e bonds. As seen before, N2 compensates the 2-fold with a highly populated LP (2.7 e). N1 shows a regular distribution with ca. 2 e bonds and LP. Finally, N3, although 3-fold coordinated leads to a highly populated bond (2.3 e) and a lowly populated LP (1.5 e). This reflects an uncomfortable geometry around this atom.

For 4N atoms, the 2N bridge arrangement shows up both in the bulk and in V1. The two extra atoms appear alternated with Si in a chain. In the bulk, Si-N bonds are in the 2-2.2e range for if further away from the bridge and smaller populations in bond closer to the 2N unit (1.7-2.0e). LPs are distributed like in the previous interstitials: N atoms in the bridge hold two small LPs (1.2-1.5 e) whereas the isolated atoms hold greater charges (up to 1.95 e). V1 leads to a highly symmetric charge distribution, with bond charges ranging 1.7-1.8 e, whereas LPs themselves are asymmetric (1.2-2.2 e). The GB structure accommodates the 4N in a 3N dendritic distribution plus 1N. Charges are rather high with the dendritic bridge structure (up to 2.3 e) and low for the terminal bonds (1.7-1.8 e). The LP distribution is regular, with 1.1-1.2 e on each N atom. For V2, nitrogen atoms are distributed forming a Si-N cycle plus one terminal N (aka N4). Charges are again rather homogeneous, with some 2.3 e bonds inside the cycle and a 1.8 e bond in N4. The nitrogen atom (N1) not showing

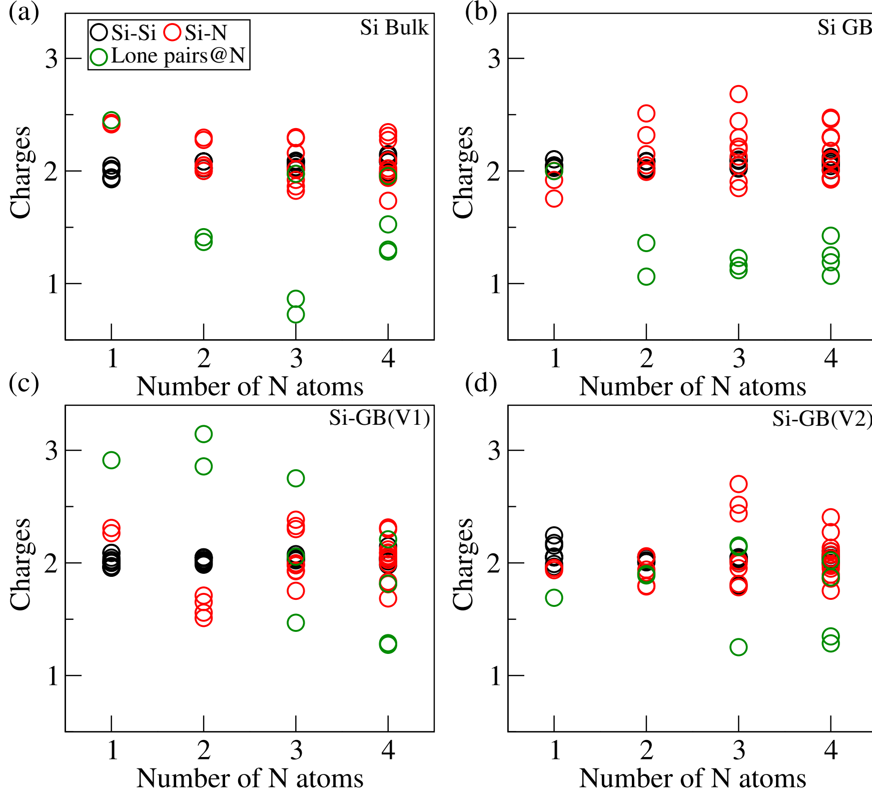

Figure 12. Bond charges (Si-Si and Si-N) and lone pairs at N (LP@N) variation for the inclusion of different numbers of nitrogen atoms in a)bulk Si b) GB c) V1 d) V2.

large bond charges compensates once again with a higherly populated LP (1.87 e) whereas the other atoms in the cycle hold 1.3 e in their LPs. The low bond charges in N4 are also compensated by 2.02 e in the lone pair (see SI: Table XX).

In general, we see that the natural coordination of N being 3, its insertion in the 4 fold structure leads to delocalized uncommon conformations (e.g. flat N coordinations). This is linked to the fact that some of these structures are gapless (see SI: Table VIII) [7]. Bond charges get far away from nominal and are compensated by LPs. This can be seen in Fig. 12, which shows the evolution of charges for different number of atoms on each structure. Lone pairs are shown in green. It can be seen that lone pairs compensate the Si-N charges, with Si-Si charges finally being little affected by the N atoms. It is worth noting that in general, a higher Si-N population is promoted, with small LP charges. There is one exception to this trend, that is V1. For V1 highly populated LPs are found for 1-3 N atoms.

D. Oxygen

In this case, the reference system is SiO_2. This structure shows bond lengths of ca. 1.62 Å, leading to bond charges in the range 1.91-1.96 e. Each oxygen atom shows two lone pairs with a total charge of 4.13 e (SI: Fig. 17). This leads to 7.98 e around each oxygen atom.

When we introduce oxygen as an interstitial, patterns are very regular. Oxygen atoms always appear in between two Si atoms, O-O bonds are never observed. Overall, this leads to structures reminiscent of SiO_2, with Si-O bonds holding ca. 1.6-1.7 e and lone pairs on the oxygen atoms. Here the lone pairs holding ca. 4.4-4.8 e, total charge close to 8 electrons (see Fig. 14) for oxygen atom.

In all cases, the insertion of oxygen atoms leads to Si-O bonds that have a slightly lower population than in bulk SiO_2 bulk. In some cases, this can go down to 1.5 e, essentially related to elongated Si-O bonds. The Si structure balances this effect, slightly increasing the Si-Si charges (Fig. 14).

Whereas two oxygen atoms always arrange linearly (Si-O-Si-O-Si), three and four oxygen atoms lead to two different arrangement types: linear (e.g. 4O in Si bulk and 3O in V1) or

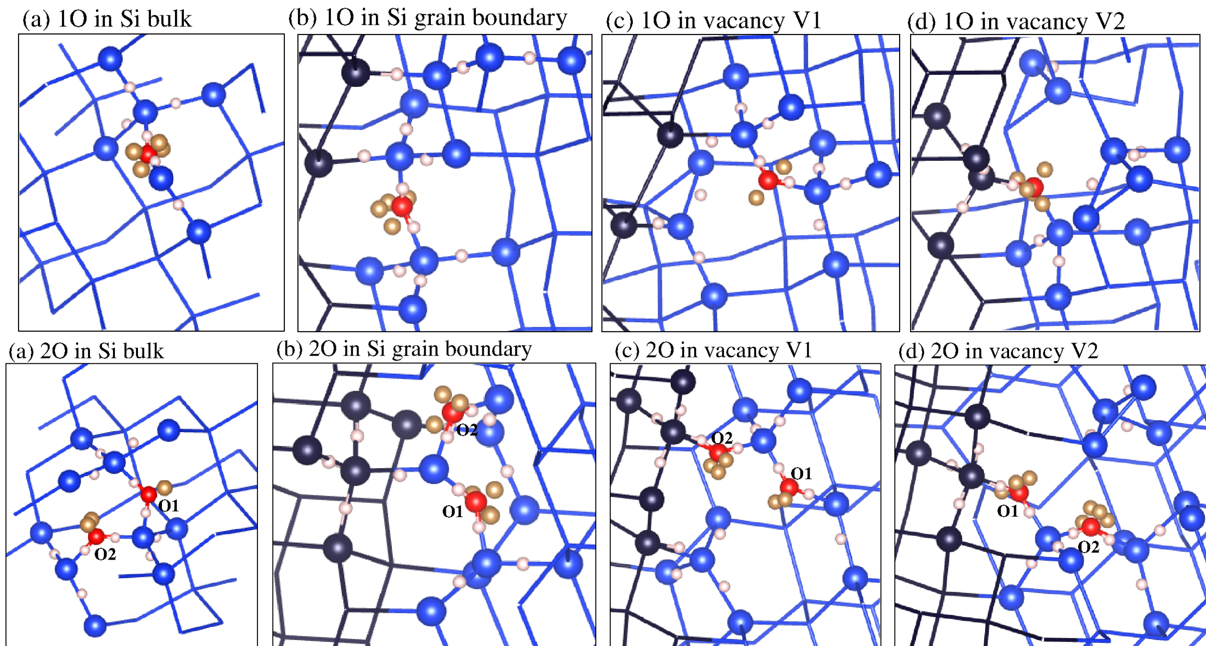

Figure 13. Structures with the inclusion of one oxygen atom (top) and two oxygen atoms (bottom) in a) bulk Si b) GB c) V1 d) V2. Silicon atoms in blue. Bonds and lone pairs are highlighted with small white spheres and brown spheres respectively

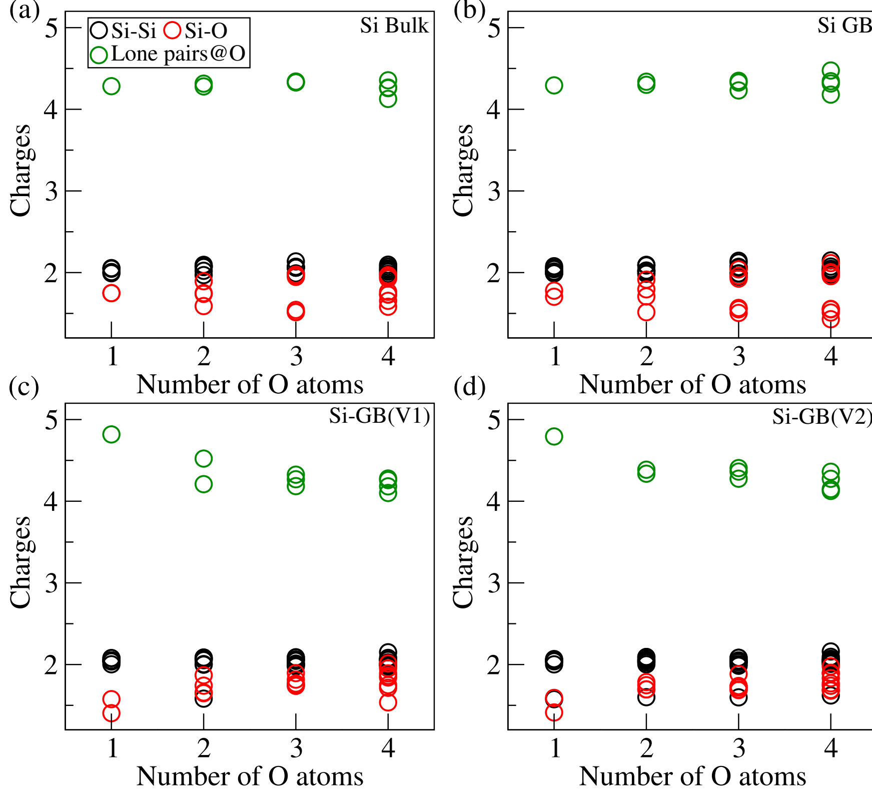

Figure 14. Bond charges (Si-Si and Si-O) and lone pairs at O (LP@O) variation with the inclusion of different numbers of oxygen atoms in a)bulk Si b) GB c) V1 d) V2.

dendritic (e.g. 3O in Si bulk) (Fig. 15). The latter usually lead to a greater Si-O charge dispersion (Fig. 14).

Fig. 14 allows to see the overall charge distribution in the different systems. Whereas the LP charges are rather stable both in the bulk and GB systems, so that the changes in Si-O bond charges are slightly compensated by the bulk, in the vacancy systems, the charge redistribution is mainly buffered within the interstitial: Si-O changes are balanced out by the LPs charge. This means that the charge on the oxygen suffers more important changes in the vacancies, with the total oxygen charge decreasing with the number of interstitials towards the bulk value. The pattern repetition leads to very linear energetic behaviors (Fig. 16 top).

IV. SUMMARY AND CONCLUSIONS

Overall, we see that the system tries to keep as much as possible the stable tetrahedral electron pair organization when defects are introduced. Grain boundaries easily stabilize

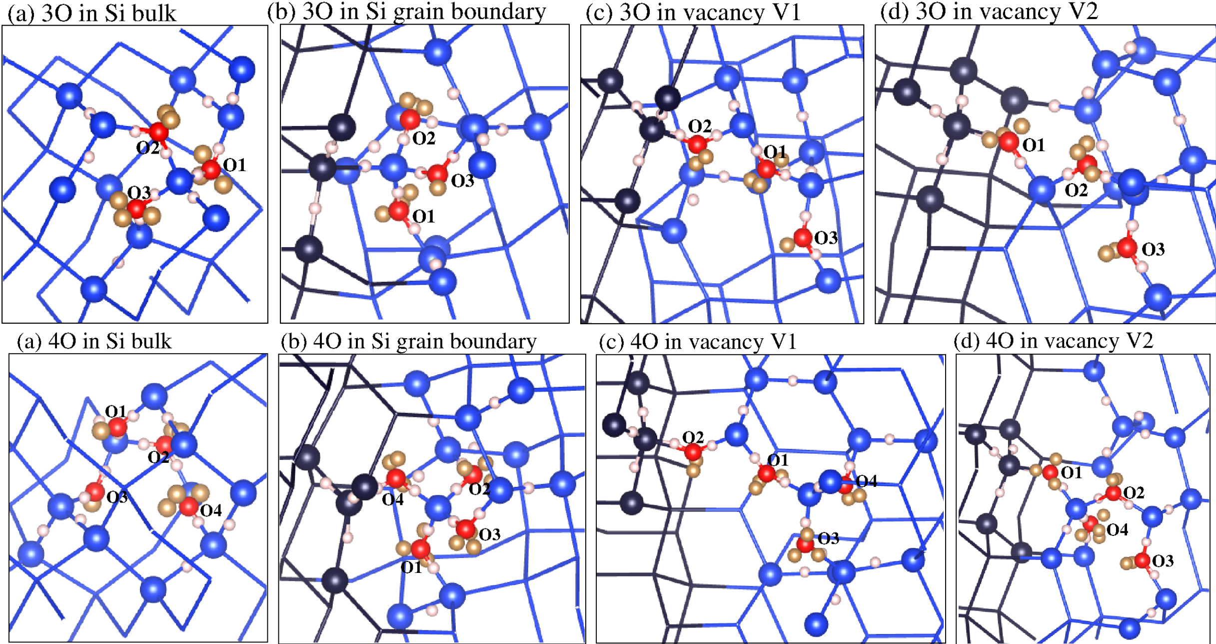

Figure 15. Structures with the inclusion of three oxygen atoms (top) and four oxygen atoms (bottom) in a) bulk Si b) GB c) V1 d) V2. Silicon atoms in blue. Bonds and lone pairs are highlighted with small white spheres and brown spheres respectively

forming new bonds at the interface. Vacancies lead to missing coordinations that are compensated by confronted lone pairs that take the position and the total charge of the missing bond. Where possible, new bonds are also formed. In this case, planar geometries and weak bonds are formed. In both cases, local deformations are needed to promote these arrangements, leading to strained bonds.

When C atoms are added as interstitials, due to the strong C-C bonds, C atoms tend to form C-based arrangements reminiscent of C-based molecules. The presence of defects lowers the formation energy, allowing for the "molecules" to be included. When there is not enough space, the C-based molecules will fit in by completing their coordination with bridges. Nevertheless, this leads to higher perturbations in the Si matrix.

The formation energy for one carbon atom changes enormously depending on the presence or not of vacancies. Indeed, ca. 3.5 eV are obtained for bulk and GB. Instead it is favorable to introduce one carbon atom in V1 and V2 ($E_{\mathrm{f}}^{\mathrm{XB}} = -1.69$ eV and -1.80 eV, respectively). This is easy to understand if we compare these systems before and after the introduction of the interstitial.

Nitrogen patterns are complex: dendrites, bridges and linear arrangements are found,

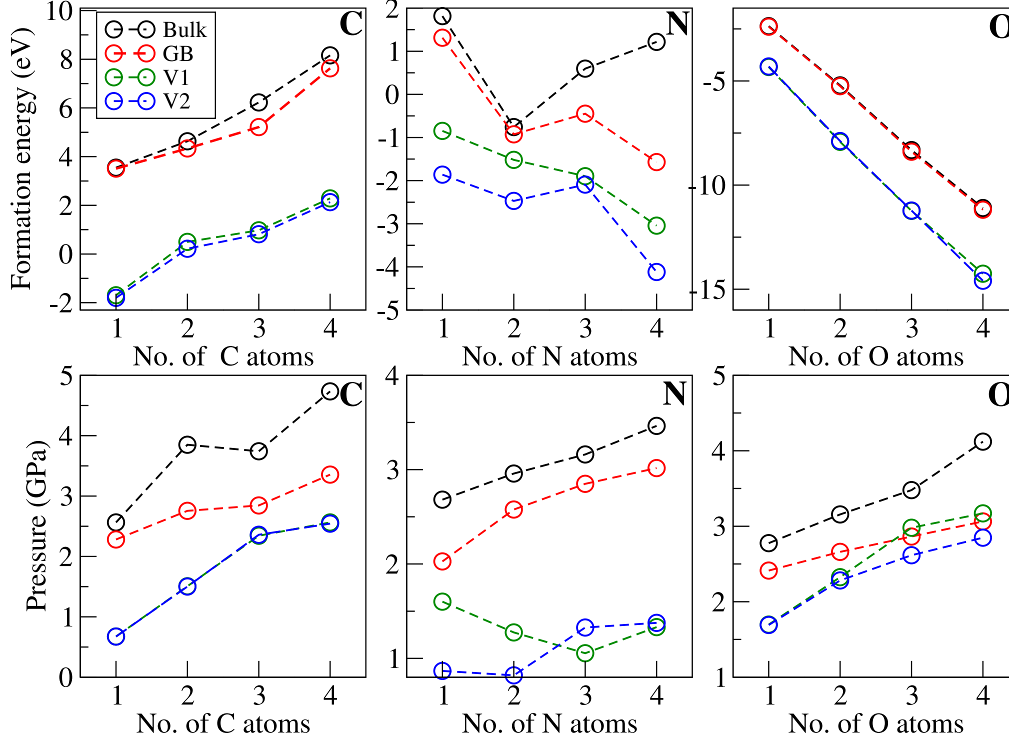

Figure 16. Formation energy variation (top) and system pressure (bottom) with the inclusion of different numbers of C/N/O impurity atoms (1 to 4) in bulk Si, GB, V1 and V2 as mentioned in legends

.

generally formed by Si-N bonds. N-N bonds are scarcely found. From the formation energy and pressure trends point of view (Fig. 16), only perceptible trends are observed for the bulk and GB pressure. This can be explained by the fact that these structures grow around the Si_2N_2 structure. Instead, vacancy structures tend to yield more dendritic organizations which, due to the sharing of bridges, induce different charge reorganizations for each new nitrogen atom.

Contrary to nitrogen, oxygen inclusions are extremely regular: Si-O very polar bonds holding 1.7-1.8 e in average and lone pairs on the Oxygen of about 4.2e (like chains of "water"). Si-O-Si arrangements are found in dendritic and linear arrangements. Overall, this pattern is rather additive, as directly reflected on the linear formation energies and pressures (Fig. 16).

ACKNOWLEDGEMENTS

We would like to thank the University of Modena and Reggio Emilia for the financial support (FAR2020 and FAR2021) and Centro Interdipartimentale En&Tech, as well as the CINECA HPC facility for the approved ISCRA C projects SiGB-NMI (IsC86_SiGB-NMI), GBimp-TS (IsC95_GBimp-TS) and Interpol (IsC90_Interpol).

---

[1] J. Neugebauer A. Pasquarello C. G. Van de Walle A. Alkauskas, P. Deák. Advanced calculations for defects in materials :electronic structure methods. 2011.

[2] N. W. Ashcroft and N. D. Mermin. Solid State Physics. Philadelphia, Pa. : Saunders college, 1976., 1976.

[3] Audrius Alkauskas, Matthew D. McCluskey, and Chris G. Van de Walle. Tutorial: Defects in semiconductors—combining experiment and theory. Journal of Applied Physics, 119(18):181101, 2016.

[4] Matthew D. McCluskey and Anderson Janotti. Defects in semiconductors. Journal of Applied Physics, 127(19):190401, 2020.

[5] G. Cantele, Elena Degoli, Eleonora Luppi, Rita Magri, D. Ninno, G. Iadonisi, and Stefano Ossicini. First-principles study of n and p doped silicon nanoclusters. Phys. Rev. B, 72:113303, Sep 2005.

[6] M. D. McCluskey and E. E. Haller. Dopants and Defects in Semiconductors. 2nd ed. CRC Press, 2018.

[7] Rita Maji, Julia Contreras-García, Nathalie Capron, Elena Degoli, and Eleonora Luppi. The role of si vacancies in the segregation of o, c, and n at silicon grain boundaries: An ab initio study. The Journal of Chemical Physics, 155:174704, 2021.

[8] Rita Maji, Eleonora Luppi, Nathalie Capron, and Elena Degoli. Ab initio study of oxygen segregation in silicon grain boundaries: The role of strain and vacancies. Acta Materialia, 204:116477, 2021.

[9] Colin A. Wolden, Juanita Kurtin, Jason B. Baxter, Ingrid Repins, Sean E. Shaheen, John T. Torvik, Angus A. Rockett, Vasilis M. Fthenakis, and Eray S. Aydil. Photovoltaic manufacturing: Present status, future prospects, and research needs. Journal of Vacuum Science &

Technology A, 29(3):030801, 2011.

[10] Peter Käshammer and Talid Sinno. Interactions of twin boundaries with intrinsic point defects and carbon in silicon. Journal of Applied Physics, 114(8):083505, 2013.

[11] Rita Maji, Julia Contreras-García, Eleonora Luppi, and Elena Degoli. Effect of strain on interactions of $\Sigma3\{111\}$ silicon grain boundary with oxygen impurities from first principles. physica status solidi (b), n/a(n/a):2100377.

[12] G. Kissinger. Oxygen impurity in crystalline silicon. In Deren Yang, editor, Handbook of Photovoltaic Silicon, pages 399-436. Springer Berlin Heidelberg, Berlin, Heidelberg, 2019.

[13] M. Pesola, J. von Boehm, T. Mattila, and R. M. Nieminen. Computational study of interstitial oxygen and vacancy-oxygen complexes in silicon. Phys. Rev. B, 60:11449-11463, Oct 1999.

[14] A. Mattoni, F. Bernardini, and L. Colombo. Self-interstitial trapping by carbon complexes in crystalline silicon. Phys. Rev. B, 66:195214, Nov 2002.

[15] Dilyara Timerkaeva, Claudio Attaccalite, Gilles Brenet, Damien Caliste, and Pascal Pochet. Structural, electronic, and optical properties of the C-C complex in bulk silicon from first principles. Journal of Applied Physics, 123(16):161421, 2018.

[16] Xuegong Yu, Deren Yang, Xiangyang Ma, Jiansong Yang, Liben Li, and Duanlin Que. Grown-in defects in nitrogen-doped czochralski silicon. Journal of Applied Physics, 92(1):188-194, 2002.

[17] Shuai Yuan and Deren Yang. Nitrogen impurity in crystalline silicon. In Deren Yang, editor, Handbook of Photovoltaic Silicon, pages 463-494. Springer Berlin Heidelberg, Berlin, Heidelberg, 2019.

[18] Zhen Zhu, Hezhu Shao, Xiao Dong, Ning Li, Bo-Yuan Ning, Xi-Jing Ning, Li Zhao, and Jun Zhuang. Electronic band structure and sub-band-gap absorption of nitrogen hyperdoped silicon. Scientific Reports, 5(10513), 2015.

[19] Julia Contreras-García, Miriam Marqués, José Manuel Menéndez, and José Manuel Recio. From elf to compressibility in solids. International Journal of Molecular Sciences, 16(4):8151-8167, 2015.

[20] Konstantinos Koumpouras and J Andreas Larsson. Distinguishing between chemical bonding and physical binding using electron localization function (ELF). Journal of Physics: Condensed Matter, 32(31):315502, may 2020.

[21] Martin Ludwig and Harald Hillebrecht. First-principles calculation of 11b solid-state nmr parameters of boron-rich compounds ii: the orthorhombic phases mgb7 and mgb12c2 and the boron modification γ-b28. Phys. Chem. Chem. Phys., 23:3883-3897, 2021.

[22] Julia Contreras-García and José Manuel Recio. Electron delocalization and bond formation under the elf framework. Theoretical Chemistry Accounts, 128:411-418, 2011.

[23] Carlo Gatti. Chemical bonding in crystals: new directions. Zeitschrift für Kristallographie - Crystalline Materials, 220(5-6):399-457, 2005.

[24] Patricio Fuentealba, E. Chamorro, and Juan C. Santos. Chapter 5 understanding and using the electron localization function. In Alejandro Toro-Labbé, editor, Theoretical Aspects of Chemical Reactivity, volume 19 of Theoretical and Computational Chemistry, pages 57-85. Elsevier, 2007.

[25] J. Contreras-García, A. Martín Pendás, J. M. Recio, and B. Silvi. Computation of local and global properties of the electron localization function topology in crystals. Journal of Chemical Theory and Computation, 5(1):164-173, Jan 2009.

[26] Feng Hao, Rickard Armiento, and Ann E. Mattsson. Using the electron localization function to correct for confinement physics in semi-local density functional theory. The Journal of Chemical Physics, 140(18):18A536, 2014.

[27] Alessandro Cossard, Silvia Casassa, Carlo Gatti, Jacques K. Desmarais, and Alessandro Erba. Topology of the electron density and of its laplacian from periodic lcao calculations on f-electron materials: The case of cesium uranyl chloride. Molecules, 26(14), 2021.

[28] Kuzmin A. Evarestov, R. A. Topological analysis of chemical bonding in the layered fepse3 upon pressure-induced phase transitions. Journal of computational chemistry, 41(31):2610–2623, 2020.

[29] Hiroshi Ogawa. Gbstudio: A builder software on periodic models of csl boundaries for molecular simulation. MATERIALS TRANSACTIONS, 47:2706–2710, 2006.

[30] Dongdong Zhao and Yanjun Li. Lattice distortion induced site dependent carbon gettering at twin boundaries in silicon. Journal of Alloys and Compounds, 712:599-604, 2017.

[31] Benedikt Ziebarth, Matous Mrovec, Christian Elsässer, and Peter Gumbsch. Interstitial iron impurities at grain boundaries in silicon: A first-principles study. Phys. Rev. B, 91:035309, 2015.

[32] G. Sarau, S. Christiansen, M. Holla, and W. Seifert. Correlating internal stresses, electrical activity and defect structure on the micrometer scale in efg silicon ribbons. Solar Energy Materials and Solar Cells, 95:2264-2271, 2011.

[33] O. H. Nielsen and Richard M. Martin. Stresses in semiconductors: Ab initio calculations on si, ge, and gaas. Phys. Rev. B, 32:3792-3805, 1985.

[34] G. Kresse and J. Hafner. Ab initio molecular dynamics for liquid metals. Phys. Rev. B, 47:558, 1993.

[35] G. Kresse and J. Furthmüller. Efficient iterative schemes for ab initio total-energy calculations using a plane-wave basis set. Phys. Rev. B, 54:11169, 1996.

[36] John P. Perdew, Kieron Burke, and Matthias Ernzerhof. Generalized gradient approximation made simple. Phys. Rev. Lett., 77:3865–3868, 1996.

[37] H. J. Monkhorst and J. D. Pack. Special points for brillouin-zone integrations. Physical Review B, 13(12):5188, 1976.

[38] Peter E. Blöchl, O. Jepsen, and O. K. Andersen. Improved tetrahedron method for brillouin-zone integrations. Phys. Rev. B, 49:16223-16233, 1994.

[39] Andrew J. Morris, Chris J. Pickard, and R. J. Needs. Hydrogen/nitrogen/oxygen defect complexes in silicon from computational searches. Phys. Rev. B, 80:144112, Oct 2009.

[40] A. Savin, O. Jepsen, J. Flad, O.K. Andersen, H. Preuss, and H. G. von Schneiring. Electron localization in solid-state structures of the elements: the diamond structure. Angew. Chem. Int. Ed. Engl., 31:187, 1997.

[41] A. D. Becke and K. E. Edgecombe. A simple measure of electron localization in atomic and molecular systems. The Journal of Chemical Physics, 92(9):5397-5403, 1990.

[42] Richard F. W. Bader. Atoms in molecules (a quantum theory). Oxford University Press, Oxford, pages 545-559, 1990.

[43] J. E. Abraham, R. H.; Marsden. Foundations of Mechanics. Addison Wesley, Reading, MA, 1994.

[44] A. Otero de-la Roza, Erin R. Johnson, and Víctor Luaña. Critic2: A program for real-space analysis of quantum chemical interactions in solids. Computer Physics Communications, 185(3):1007-1018, 2014.

SUPPORTING INFORMATION

Bulk systems

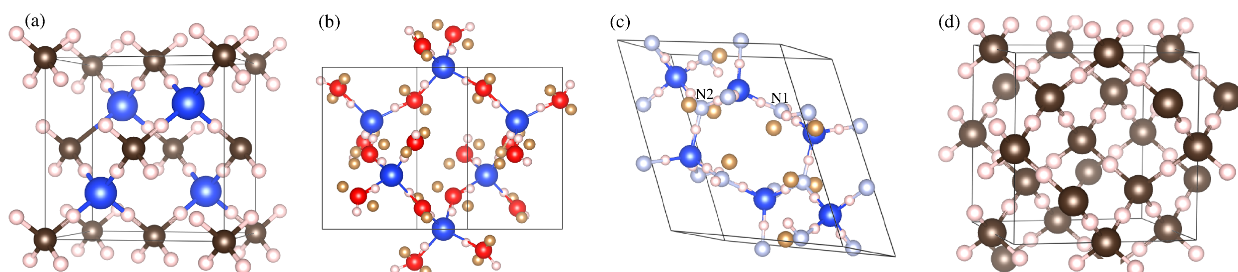

Figure 17. a) SiC b) SiO_2 c) Si_3N_4 d)Diamond

	Si	SiC	SiO_2	Si_3N_4	Diamond
Bond Charges(BC)	1.999	2.000	1.908, 1.957	2.313	1.999
Bond length(BL)Å	2.351	1.896	1.625, 1.628	1.747	1.547
Lone Pair(LP)			4.1340	N2:(0.5289 each) 1.0578	

Table I. References from bulk systems

Molecular systems

	Ethane	Ethylene	Cyclopropane	Cyclopropene	Bicyclobutane
Bond Charges(BC)	1.81	3.42	1.70	1.80, 3.20	1.87, 1.72
Bond length(BL)Å	1.53	1.33	1.52	1.53, 1.30	1.46, 1.55

Table II. References from molecular systems

	Bond Charges(BC)	Bond length(BL)Å	LP
Si-GB	2.00329	2.35084	
	2.00096	2.35122	
	1.98795	2.36642	
Si-GB: V1	2.0697	2.32564	Si1: 0.99
	2.0138	2.37601	Si2: 1.00
	2.0138	2.37601	
	2.0192	2.36607	
	2.0192	2.36607	
	2.0712	2.31773	
	2.0712	2.31773	
	1.9712	2.42741	
	2.0282	2.47125	
	2.0062	2.50193	
	2.0280	2.31424	
	2.0280	2.31424	
	1.5429	2.45097	
Si-GB: V2	2.0172	2.37177	Si1: 0.97
	2.0172	2.37177	Si2: 1.03
	2.0609	2.32423	
	2.0609	2.32423	
	2.0676	2.32906	
	2.0676	2.32906	
	1.9926	2.35628	
	1.9782	2.43172	
	2.0207	2.43038	
	2.0207	2.43038	
	2.0273	2.48162	
	2.0251	2.31610	
	1.5522	2.44485	

Table III. References from GB

X	$E_{\mathrm{f}}^{\mathrm{XB}}$	$E_{\mathrm{f}}^{\mathrm{XGB}}$	$E_{\mathrm{f}}^{\mathrm{XV1GB}}$	$E_{\mathrm{f}}^{\mathrm{XV2GB}}$
1C	3.5467	3.5072	-1.6935	-1.8003
2C	4.6315	4.3359	0.4985	0.2165
3C	6.2242	5.2122	0.9758	0.8144
4C	8.1596	7.6275	2.2861	2.1306

Table IV. Formation energy (eV) of Si bulk and $\Sigma3\{111\}$ Si GB without/with vacancies V1 and V2 with interstitial C atoms from 1 to 4. The values are reported for the lowest energy structures.

X	$E_g^{\text{Si-bulk}}$	E_g^{GB}	E_g^{V1GB}	E_g^{V2GB}
1C	0	0.0477	0.3587	0.4014
2C	0.4291	0.5235	0	0
3C	0.6944	0.4729	0.6066	0.5578
4C	0.4549	0.1319	0.6502	0.5978

Table V. Energy gaps (eV) of Si bulk and $\Sigma 3\{111\}$ Si GB without/with vacancies V1 and V2 with interstitial C atoms from 1 to 4. The values are reported for the lowest energy structures.

X	P(X+B)	P(X+GB)	P(X+V1GB)	P(X+V2GB)
1C	2.564	2.281	0.674	0.673
2C	3.850	2.756	1.507	1.502
3C	3.742	2.845	2.343	2.359
4C	4.734	3.356	2.563	2.543

Table VI. Hydrostatic pressure (GPa) of Si bulk and $\Sigma 3\{111\}$ Si GB without/with vacancies V1 and V2 with interstitial C atoms from 1 to 4. The values are reported for the lowest energy structures.

X	E_f^{XB}	E_f^{XGB}	E_f^{XV1GB}	E_f^{XV2GB}
1N	1.8155	1.3127	-0.8477	-1.8618
2N	-0.7577	-0.9272	-1.5182	-2.4698
3N	0.5968	-0.4488	-1.8968	-2.0912
4N	1.2163	-1.5700	-3.0445	-4.1177

Table VII. Formation energy (eV) of Si bulk and $\Sigma 3\{111\}$ Si GB without/with vacancies V1 and V2 with interstitial N atoms from 1 to 4. The values are reported for the lowest energy structures.

X	$E_g^{\text{Si-bulk}}$	E_g^{GB}	E_g^{V1GB}	E_g^{V2GB}
1N	0	0	0	0
2N	0.5427	0.5444	0.2439	0.6191
3N	0	0	0	0
4N	0.3464	0.6274	0.3966	0.6397

Table VIII. Energy gaps (eV) of Si bulk and $\Sigma 3\{111\}$ Si GB without/with vacancies V1 and V2 with interstitial N atoms from 1 to 4. The values are reported for the lowest energy structures.

X	P(X+B)	P(X+GB)	P(X+V1GB)	P(X+V2GB)
1N	2.682	2.027	1.601	0.867
2N	2.959	2.577	1.275	0.820
3N	3.161	2.850	1.054	1.327
4N	3.464	3.017	1.331	1.376

Table IX. Hydrostatic pressure (GPa) of Si bulk and Σ3{111} Si GB without/with vacancies V1 and V2 with interstitial N atoms from 1 to 4. The values are reported for the lowest energy structures.

X	$E_{\mathrm{f}}^{\mathrm{XB}}$	$E_{\mathrm{f}}^{\mathrm{XGB}}$	$E_{\mathrm{f}}^{\mathrm{XV1GB}}$	$E_{\mathrm{f}}^{\mathrm{XV2GB}}$
1O	-2.3649	-2.3950	-4.3281	-4.3036
2O	-5.2126	-5.2515	-7.9224	-7.8855
3O	-8.3195	-8.3974	-11.2368	-11.2213
4O	-11.0994	-11.1843	-14.2579	-14.5924

Table X. Formation energy (eV) of Si bulk and Σ3{111} Si GB without/with vacancies V1 and V2 with interstitial O atoms from 1 to 4. The values are reported for the lowest energy structures.

X	$E_{\mathrm{g}}^{\mathrm{Si\text{-}bulk}}$	$E_{\mathrm{g}}^{\mathrm{GB}}$	$E_{\mathrm{g}}^{\mathrm{V1GB}}$	$E_{\mathrm{g}}^{\mathrm{V2GB}}$
1O	0.6086	0.5506	0.6274	0.6283
2O	0.5913	0.6073	0.6353	0.6292
3O	0.7285	0.6185	0.6306	0.6319
4O	0.7430	0.5569	0.6850	0.6989

Table XI. Energy gaps (eV) of Si bulk and Σ3{111} Si GB without/with vacancies V1 and V2 with interstitial O atoms from 1 to 4. The values are reported for the lowest energy structures.

X	P(X+B)	P(X+GB)	P(X+V1GB)	P(X+V2GB)
1O	2.776	2.413	1.697	1.692
2O	3.157	2.660	2.325	2.282
3O	3.479	2.864	2.981	2.616
4O	4.121	3.064	3.171	2.849

Table XII. Hydrostatic pressure (GPa) of Si bulk and Σ3{111} Si GB without/with vacancies V1 and V2 with interstitial O atoms from 1 to 4. The values are reported for the lowest energy structures.

Si-Bulk	BC(Si-Si)	BL(Si-Si)Å	BC(Si-C)	BL(Si-C)Å	BC(C-C)	BL(C-C)Å	LP
1C	1.9917	2.31736	2.4598	1.81289			0.14269
	1.9916	2.31759	2.5371	1.81233			
	1.9950	2.31807	2.3758	1.74694			
	1.9948	2.31842					
	2.2328	2.28068					
	2.2350	2.28173					
	1.9995	2.44675					
2C	1.9779	2.31447	2.4845	1.78563	3.0651	1.31413	
	1.9781	2.31436	2.4843	1.78585			
	1.9779	2.31428	1.7554	1.84197			
	1.9782	2.31450	1.7557	1.84192			
	2.1463	2.25425					
	2.1460	2.25412					
	1.9930	2.30624					
3C	2.0201	2.31590	2.3825	1.81499	1.5792	1.53572	
	2.0046	2.30954	2.3820	1.81535	1.5777	1.53568	
	2.0047	2.30951	1.9941	1.87728	1.41599	1.50008	
	2.0202	2.31584	1.9021	1.87268			
	2.0693	2.34550	1.9028	1.87244			
	2.0693	2.28606					
	2.1675	2.20866					
	1.9581	2.34297					
	1.9577	2.34290					
4C	1.9954	2.36665	2.2361	1.84433	2.1508	1.41648	C3: 0.01604
	2.0178	2.32830	2.3127	1.80898	3.0399	1.34593	
	2.0250	2.38233	2.2938	1.85218	1.7943	1.46732	
	2.0650	2.26366	2.3754	1.81756	1.0551	1.66790	
	2.0407	2.28754	1.9845	1.86359			
	1.9946	2.30892	2.1936	1.87557			
	1.9880	2.31720					
	1.9545	2.34714					
	1.9410	2.35165					

Table XIII. Bond charge(BC), bond length (BL) and lone pair(LP) data for Si-Si, Si-C and C-C bonds with the inclusion of n numbers of C atoms (n=1,2,3 & 4) in Si-bulk.

Si-GB	BC(Si-Si)	BL(Si-Si)Å	BC(Si-C)	BL(Si-C)Å	BC(C-C)	BL(C-C)Å	LP
1C	1.9903	2.31786	2.2747	1.81425			0.5948
	2.0164	2.31981	2.2497	1.81470			
	1.9814	2.31807	2.4034	1.74762			
	2.2083	2.29283					
	2.0041	2.33252					
	2.2183	2.29363					
	2.0015	2.45067					
2C	2.0507	2.37415	2.3492	1.83840	2.8306	1.37792	
	2.0595	2.36930	2.3430	1.84499			
	2.0793	2.27725	2.1074	1.86866			
	2.0129	2.29788	2.1091	1.86785			
	2.0158	2.29966					
	1.9780	2.34655					
	1.9662	2.35109					
	2.0841	2.26822					
	2.0117	2.34787					
	1.9379	2.31357					
3C	2.0549	2.42702	2.2420	1.85243	1.5274	1.57712	C3: 0.001514
	2.0493	2.30263	2.2603	1.85057			
	2.0167	2.33603	2.2152	1.84016			
	2.0128	2.33161	2.1312	1.85078			
	2.0341	2.35625	2.1595	1.84555			
	2.0395	2.32409	1.8675	1.93941			
	2.0554	2.44381	1.8601	1.93139			
	1.9637	2.32060	1.8795	1.88733			
	2.2222	2.21525	1.6191	1.88109			
			1.5615	1.89062			
4C	2.0053	2.31422	2.3129	1.83722	2.5353	1.39499	
	2.0744	2.32324	2.2215	1.87488			
	2.0044	2.33814	2.1408	1.89536			
	2.0281	2.36433	2.4743	1.78531			
	1.9727	2.34566	2.4729	1.78473			
	1.9471	2.32925	2.4820	1.80381			
	1.8315	2.48968	2.5122	1.77339			
	1.8336	2.44290	2.1517	1.79929			
	1.1289	2.57283	2.7127	1.75854			
			1.7269	1.95371			
			1.1668	2.03012			

Table XIV. Bond charge(BC), bond length (BL) and lone pair(LP) data for Si-Si, Si-C and C-C bonds with the inclusion of n numbers of C atoms (n=1,2,3 & 4) in Si-GB

	Si-VGB	BC(Si-Si)	BL(Si-Si)Å	BC(Si-C)	BL(Si-C)Å	BC(C-C)	BL(C-C)Å	LP
	1C	2.0243	2.39351	1.9629	1.99583			
		2.0242	2.39361	1.9526	2.00851			
		2.0205	2.39538	1.9201	2.03954			
		2.0289	2.39751	1.9199	2.03983			
		2.0210	2.40463					
		2.0211	2.40463					
		2.0291	2.39740					
		2.0115	2.34935					
		2.0237	2.40396					
		2.0115	2.34945					
		2.0238	2.40392					
		1.9847	2.34152					
		2.0026	2.46212					
		1.9689	2.42414					
V1	2C	2.0236	2.40835	2.4013	1.88745	2.3241	1.41529	
		2.0234	2.42022	2.4174	1.88984			
		2.0299	2.42408	2.4146	1.88913			
		2.0176	2.42635	2.4217	1.88409			
		2.0019	2.33929					
		2.0023	2.34743					
		2.0037	2.34256					
		1.9859	2.37766					
		1.9560	2.37192					
		1.9545	2.37375					
	3C	2.0355	2.32286	2.6560	1.80175	3.0039	1.31195	
		2.0148	2.39841	2.7033	1.80450	1.5660	1.51629	
		2.0329	2.29982	2.1869	1.89111	1.5181	1.52702	
		2.0273	2.33162	2.1780	1.90020			
		2.0332	2.32608					
		1.9774	2.32650					
		1.9799	2.34479					
		1.9779	2.34151					
		2.0099	2.42987					
		1.9848	2.31307					
		1.9863	2.37639					
		1.9979	2.37766					
		1.9875	2.37762					
	4C	2.0668	2.30703	2.3035	1.85418	1.6203	1.53713	C1: 0.010741
		2.0139	2.31936	2.5360	1.83508	1.6193	1.53703	C3: 0.035845
		2.0058	2.34112	2.5114	1.83507	1.5869	1.55733	C3: 0.021072
		2.0131	2.34511	2.3171	1.85991	1.5648	1.55739	
		2.0274	2.37703	2.0619	1.84544	1.3678	1.46903	
		2.0276	2.37684	2.0494	1.90386			
		2.0429	2.35443					
		2.0429	2.35446					
		2.0115	2.29645					
		2.0414	2.36713					

Table XV. Bond charge(BC), bond length (BL) and lone pair(LP) data for Si-Si, Si-C and C-C bonds with the inclusion of n numbers of C atoms (n=1,2,3 & 4) in Si-GB with vacancy V1.

	Si-VGB	BC(Si-Si)	BL(Si-Si)Å	BC(Si-C)	BL(Si-C)Å	BC(C-C)	BL(C-C)Å	LP
V2	1C	2.0281	2.38089	1.9623	2.00709			
		2.0281	2.38089	1.9271	2.01777			
		2.0184	2.38908	1.9333	2.03516			
		2.0207	2.40451	1.9333	2.03516			
		2.0207	2.40451					
		2.0272	2.39927					
		2.0272	2.39927					
		2.0224	2.39941					
		2.0224	2.39941					
		2.0196	2.39996					
		2.0022	2.46209					
		2.0022	2.46209					
	2C	2.0119	2.32572	2.3918	1.89263	2.3152	1.41603	
		2.0235	2.40835	2.4065	1.89224			
		2.0171	2.42459	2.4949	1.87145			
		2.0034	2.32550	2.4071	1.88101			
		1.9984	2.38682					
		1.9612	2.35986					
		1.9912	2.33270					
		1.9641	2.41901					
		1.9530	2.37274					
		1.9518	2.37180					
	3C	2.0037	2.33228	2.6418	1.80187	2.9989	1.31248	
		1.9961	2.33392	2.7338	1.79859	1.5669	1.51368	
		1.9890	2.33664	2.1864	1.89848	1.5185	1.52813	
		2.0321	2.30156	2.1773	1.90683			
		2.0308	2.33111					
		2.0230	2.32828					
		2.0121	2.41445					
		2.0278	2.32947					
	4C	2.0689	2.31040	2.2894	1.86170	1.6442	1.53314	
		2.0040	2.33369	2.5498	1.83354	1.6105	1.53866	
		1.9870	2.32764	2.5521	1.84761	1.5948	1.55655	
		2.0023	2.33598	2.3272	1.86247	1.5870	1.55328	
		2.0042	2.33820	2.0410	1.84755	1.3498	1.47835	
		2.0345	2.35649	2.0608	1.90940			
		2.0533	2.31292					
		2.0063	2.33383					
		2.0353	2.34643					

Table XVI. Bond charge(BC), bond length (BL) and lone pair(LP) data for Si-Si, Si-C and C-C bonds with the inclusion of n numbers of C atoms (n=1,2,3 & 4) in Si-GB with vacancy V2.

Si-Bulk	BC(Si-Si)	BL(Si-Si)Å	BC(Si-N)	BL(Si-N)Å	BC(N-N)	BL(N-N)Å	LP
1N	2.0478 1.9314 1.9270 2.0029 2.0013 2.0181 1.9412 1.9427	2.33613 2.32035 2.32165 2.35253 2.35318 2.35985 2.33676 2.33660	2.4274 2.4141	1.66719 1.66703			2.4509
2N	2.0849 2.0843 2.0843 2.0849 2.0244 2.0239	2.30713 2.30644 2.30645 2.30701 2.31767 2.31746	2.2752 2.2956 2.0008 2.0007 2.0293 2.0508	1.73464 1.73455 1.73999 1.73986 1.76801 1.76801			N1: 1.4121 N2: 1.3700
3N	2.0352 2.0792 2.0869 2.0827 2.0912 2.0617 2.0273 2.0109	2.28999 2.30490 2.31795 2.33198 2.30624 2.28782 2.31692 2.31369	2.2909 2.3008 1.9742 2.0136 1.9209 2.1595 1.8634 2.0166 1.8249	1.73687 1.73777 1.74611 1.74460 1.76536 1.76647 1.73632 1.76668 1.78669			N1: 0.7259 N2: 0.8651 N3: 1.9743
4N	2.0829 2.0801 2.0871 2.1036 2.1494 2.1334 1.9851	2.33553 2.32301 2.29693 2.30566 2.25315 2.35389 2.30198	2.3121 2.3443 2.0021 2.0234 1.9686 1.9389 2.2747 1.9527 2.0948 2.0943 1.9726 1.7351	1.73744 1.71281 1.75323 1.74916 1.75665 1.77627 1.72530 1.74615 1.76061 1.77118 1.73255 1.76306			N1: 1.2854 N2: 1.3015 N3: 1.5256 N4: 1.9553

Table XVII. Bond charge(BC), bond length (BL) and lone pair(LP) data for Si-Si, Si-N and N-N bonds with the inclusion of n numbers of N atoms (n=1,2,3 & 4) in Si-bulk.

Si-GB	BC(Si-Si)	BL(Si-Si)Å	BC(Si-N)	BL(Si-N)Å	BC(N-N)	BL(N-N)Å	LP
1N	2.0376	2.32647	2.0010	1.76298			1.9985
	2.0375	2.32636	1.9200	1.74187			
	2.0492	2.32064	1.7552	1.76611			
	2.0493	2.32045					
	2.0331	2.45711					
	2.1035	2.31514					
	2.1035	2.31462					
	2.0271	2.43737					
2N	2.0834	2.31385	2.3180	1.73044			N1: 1.3607
	2.0832	2.31385	2.5108	1.72975			N2: 1.0621
	2.0883	2.31135	2.1484	1.74457			
	2.0881	2.31135	2.0497	1.74220			
	2.0104	2.31162	1.9979	1.77111			
	2.0247	2.32479	1.9923	1.76485			
3N	2.1013	2.29004	2.1939	1.74968			N1: 1.1192
	2.0927	2.31424	2.2970	1.72659			N2: 1.2278
	2.0902	2.30417	2.6832	1.71560			N3: 1.1573
	2.0275	2.32465	2.4427	1.74610			
	2.0207	2.33297	2.2157	1.74352			
	2.0532	2.35819	2.1275	1.73394			
			2.0487	1.71729			
			1.8478	1.75508			
			1.9054	1.79481			
4N	2.1249	2.27680	2.4731	1.73868			N1: 1.4252
	2.0931	2.30091	2.1082	1.76076			N2: 1.0691
	2.0432	2.30684	2.3015	1.72478			N3: 1.1897
	2.0634	2.30310	2.4608	1.72397			N4: 1.2506
	2.0821	2.34419	2.3014	1.74044			
	2.0068	2.31122	2.0111	1.75477			
			2.1785	1.74475			
			2.2933	1.78921			
			1.9397	1.77425			
			2.0967	1.73882			
			1.9236	1.77890			
			1.9361	1.77797			

Table XVIII. Bond charge(BC), bond length (BL) and lone pair(LP) data for Si-Si, Si-N and N-N bonds with the inclusion of n numbers of N atoms (n=1,2,3 & 4) in Si-GB.

	Si-VGB	BC(Si-Si)	BL(Si-Si)Å	BC(Si-N)	BL(Si-N)Å	BC(N-N)	BL(N-N)Å	LP
	1N	2.0247	2.41953	2.3100	1.69449			2.9121
		2.0197	2.43623	2.2639	1.69582			
		2.0010	2.35263					
		2.0038	2.34135					
		2.0009	2.35266					
		1.9653	2.38943					
		1.9649	2.38938					
		2.0462	2.30787					
		1.9577	2.38419					
		1.9570	2.38426					
		2.0887	2.32091					
		2.0894	2.31500					
		1.9718	2.30958					
V1	2N	2.0434	2.34686	1.7099	1.80391	1.0824	1.45049	N1: 2.8568
		2.0256	2.41936	1.6528	1.80577			N2: 3.1440
		2.0453	2.34935	1.5105	1.83934			
		2.0452	2.34960	1.5587	1.83902			
		2.0501	2.33689					
		2.0484	2.35730					
		2.0241	2.44403					
		2.0094	2.34903					
		1.9838	2.33999					
		1.9960	2.55257					
	3N	2.0773	2.41155	2.3000	1.73292			N1: 2.0548
		2.0422	2.37194	1.9799	1.82098			N2: 2.7514
		2.0225	2.33420	1.9268	1.78660			N3: 1.4688
		2.0439	2.40624	2.3839	1.68197			
		1.9813	2.31695	1.9969	1.79269			
		2.0262	2.37227	2.3275	1.70177			
		2.0281	2.42340	1.9324	1.81505			
		2.0372	2.40966	1.7521	1.84096			
		2.0574	2.48591					
	4N	2.1485	2.46424	2.0854	1.74349			N1: 1.8152
		2.0467	2.35171	2.0270	1.73643			N2: 1.2873
		2.0365	2.42135	2.0928	1.77086			N3: 1.2731
		2.0349	2.38921	2.1196	1.75251			N4: 2.2097
		2.0348	2.41911	1.9919	1.77712			
		2.0138	2.36413	2.0611	1.79525			
		1.9812	2.32272	2.0450	1.79535			
		2.0344	2.49119	1.8110	1.76966			
				2.2998	1.80866			
				1.8331	1.84124			
				2.3149	1.77682			
				1.6849	1.80845			

Table XIX. Bond charge(BC), bond length (BL) and lone pair(LP) data for Si-Si, Si-N and N-N bonds with the inclusion of n numbers of N atoms (n=1,2,3 & 4) in Si-GB with vacancy V1.

	Si-VGB	BC(Si-Si)	BL(Si-Si)Å	BC(Si-N)	BL(Si-N)Å	BC(N-N)	BL(N-N)Å	LP
	1N	2.0564	2.36784	1.9553	1.87247			N: 1.6904
		2.0509	2.40413	1.9558	1.87367			Si: 0.4432
		2.0493	2.40528	1.9353	1.86030			
		2.0511	2.38624					
		2.0483	2.38886					
		1.9908	2.40434					
		1.9654	2.40723					
		2.1537	2.33401					
		2.1767	2.33784					
		2.2444	2.32922					
V2	2N	2.0061	2.31947	2.0590	1.76352			N1: 1.8892
		2.0063	2.31967	2.0490	1.76331			N2: 1.9015
		2.0476	2.36605	1.9409	1.80508			
		2.0227	2.33318	1.9121	1.80526			
		2.0426	2.45558	1.7975	1.82537			
		2.0550	2.53332	1.7913	1.82514			
		2.0549	2.53382					
	3N	2.0252	2.36235	2.4391	1.75975			N1: 1.2519
		2.0156	2.33604	1.9526	1.77458			N2: 2.1413
		2.0422	2.35106	2.7003	1.65230			N3: 2.1548
		2.0451	2.35443	1.9947	1.77620			
		2.0241	2.38609	2.0178	1.78340			
		2.0507	2.43521	2.5160	1.66644			
		2.0473	2.41717	1.8130	1.79287			
		2.0488	2.51035	1.7839	1.81480			
		2.0415	2.51595					
		1.7991	2.35569					
	4N	2.0319	2.28568	2.2734	1.73678			N1: 1.8719
		2.1039	2.42680	2.1041	1.75573			N2: 1.3477
		2.0438	2.26015	2.1349	1.76866			N3: 1.2853
		2.0431	2.35302	2.0410	1.74235			N4: 2.0208
		2.0439	2.35439	2.4054	1.75972			
		2.0269	2.37705	1.9884	1.77301			
		1.9962	2.33643	2.0737	1.76081			
		2.0385	2.42899	1.9729	1.78870			
		2.0439	2.42410	1.8965	1.77478			
		2.0702	2.47255	1.9491	1.77956			
		2.0709	2.51903	1.8610	1.79077			
		2.0000	2.46747	1.7530	1.80498			

Table XX. Bond charge(BC), bond length (BL) and lone pair(LP) data for Si-Si, Si-N and N-N bonds with the inclusion of n numbers of N atoms (n=1,2,3 & 4) in Si-GB with vacancy V2.

Si-Bulk	BC(Si-Si)	BL(Si-Si)Å	BC(Si-O)	BL(Si-O)Å	LP
1O	1.9918	2.32115	1.7489	1.63550	O1: 4.283
	2.0069	2.32194	1.7479	1.63423	
	2.0467	2.32461			
	2.0555	2.32523			
2O	2.0789	2.30065	1.8939	1.64273	O1: 4.2801
	2.0795	2.30074	1.7391	1.66098	O2: 4.3145
	2.0221	2.32101	1.7493	1.63986	
	1.9685	2.31220	1.5902	1.67594	
	2.0680	2.33876			
	2.0681	2.33886			
	2.0950	2.33589			
3O	2.1373	2.24814	1.9606	1.62698	O1: 4.3299
	1.9904	2.30827	1.9473	1.62684	O2: 4.3404
	2.0606	2.33173	1.9752	1.62684	O3: 4.3299
	2.0602	2.33169	1.5148	1.68729	
	2.0598	2.33175	1.5429	1.68740	
	2.0714	2.35013	1.5191	1.68737	
	2.0710	2.34967			
4O	2.0971	2.22921	1.9675	1.63190	O1: 4.2585
	2.0108	2.32069	1.9450	1.62957	O2: 4.1269
	2.0322	2.32228	1.9281	1.62211	O3: 4.2659
	1.9837	2.30422	1.7651	1.66014	O4: 4.3555
	2.0497	2.33004	1.7301	1.63470	
	2.0734	2.34109	1.7331	1.65317	
			1.6537	1.66647	
			1.5824	1.68762	

Table XXI. Bond charge(BC), bond length (BL) and lone pair(LP) data for Si-Si and Si-O bonds with the inclusion of n numbers of O atoms (n=1,2,3 & 4) in Si-bulk.

Si-GB	BC(Si-Si)	BL(Si-Si)Å	BC(Si-O)	BL(Si-O)Å	LP
1O	2.0093	2.32532	1.7792	1.63913	4.2934
	1.9902	2.32383	1.7035	1.63789	
	2.0134	2.33911			
	2.0425	2.32990			
	2.0564	2.32704			
	2.0781	2.32612			
	1.9997	2.32640			
	1.9931	2.34696			
	1.9959	2.36746			
2O	2.0872	2.31206	1.9142	1.64514	O1: 4.3003
	2.0250	2.32108	1.7951	1.64091	O2: 4.3380
	2.0197	2.32159	1.7078	1.66111	
	2.0920	2.31034	1.5149	1.67498	
	2.0950	2.33289			
	2.0132	2.35452			
	2.0226	2.32704			
	1.9877	2.36383			
	1.9847	2.32704			
	1.9957	2.35741			
3O	2.1448	2.25427	1.9600	1.62934	O1: 4.2309
	2.1231	2.28737	2.0395	1.62583	O2: 4.3284
	2.0699	2.34079	1.9255	1.63628	O3: 4.3491
	2.0687	2.36253	1.5670	1.68212	
	2.0445	2.33292	1.5497	1.68240	
	2.0624	2.34653	1.5057	1.69960	
	1.9502	2.32814			
	1.9914	2.33156			
	1.9873	2.33906			
4O	1.9968	2.30698	2.1162	1.60775	O1: 4.1798
	2.0109	2.31411	1.9557	1.60825	O2: 4.3162
	2.0089	2.29839	2.0040	1.60321	O3: 4.4751
	2.0324	2.32370	1.9907	1.61242	O4: 4.3444
	2.0459	2.36708	1.5109	1.69476	
	2.0352	2.32384	1.5546	1.69474	
	2.0739	2.37431	1.5502	1.69645	
	2.1489	2.29031	1.4290	1.71093	
	1.9766	2.33417			

Table XXII. Bond charge(BC), bond length (BL) and lone pair(LP) data for Si-Si and Si-O bonds with the inclusion of n numbers of O atoms (n=1,2,3 & 4) in Si-GB

	Si-VGB	BC(Si-Si)	BL(Si-Si)Å	BC(Si-O)	BL(Si-O)Å	LP
V1	1O	2.0433	2.35933	1.5763	1.70276	4.8177
		2.0432	2.35930	1.4038	1.70352	
		2.0504	2.34937			
		2.0503	2.34933			
		2.0493	2.41995			
		2.0374	2.44706			
		2.0781	2.32314			
		2.0788	2.31593			
		2.0029	2.31171			
	2O	2.0854	2.34609	1.8687	1.63189	O1: 4.5218
		2.0853	2.34610	1.6492	1.68177	O2: 4.2086
		1.9984	2.31011	1.7409	1.66199	
		2.0531	2.38759	1.6583	1.66506	
		2.0612	2.35561			
		2.0613	2.35561			
		2.0745	2.32627			
		2.0759	2.32289			
		2.0046	2.31500			
		1.5825	2.45085			
	3O	2.0851	2.31788	1.8948	1.62656	O1: 4.2695
		2.0886	2.32236	1.8150	1.63978	O2: 4.1855
		2.0016	2.31408	1.7386	1.62749	O3: 4.3248
		2.0592	2.34710	1.7672	1.63987	
		2.0592	2.34711	1.7558	1.65652	
		2.0446	2.31293	1.7408	1.65403	
		2.0107	2.32353			
		1.9913	2.34144			
		1.9769	2.33572			
		2.0050	2.31155			
	4O	2.1503	2.27352	2.0133	1.62843	O1: 4.1015
		2.0809	2.31442	1.8618	1.62652	O2: 4.1822
		2.0001	2.31435	1.8409	1.64666	O3: 4.2785
		1.9944	2.30186	1.7146	1.66121	O4: 4.2594
		2.0569	2.32987	1.9526	1.62095	
		2.0262	2.30338	1.8908	1.62452	
		2.0582	2.34486	1.7483	1.65339	
		2.0608	2.34711	1.5363	1.69373	
		2.0576	2.38358			
		2.0007	2.33742			
		1.9774	2.34089			

Table XXIII. Bond charge(BC), bond length (BL) and lone pair(LP) data for Si-Si and Si-O bonds with the inclusion of n numbers of O atoms (n=1,2,3 & 4) in Si-GB with vacancy V1.

	Si-VGB	BC(Si-Si)	BL(Si-Si)Å	BC(Si-O)	BL(Si-O)Å	LP
V2	1O	2.0490	2.35202	1.5907	1.70536	4.7927
		2.0490	2.35202	1.4133	1.70324	
		2.0389	2.34423			
		2.0479	2.39899			
		2.0479	2.39899			
		2.0459	2.42851			
		2.0673	2.32292			
		2.0017	2.31335			
		1.5752	2.43705			
	2O	2.0916	2.34935	1.7851	1.63329	O1: 4.3862
		2.0916	2.34935	1.6953	1.66673	O2: 4.3375
		2.0257	2.32115	1.7470	1.68194	
		2.0257	2.32115	1.6959	1.66639	
		2.0504	2.36999			
		2.0504	2.36999			
		2.0360	2.33241			
		2.0735	2.37747			
		2.0611	2.32703			
		2.0018	2.31163			
		1.6003	2.43229			
	3O	2.0823	2.30486	1.8844	1.65237	O1: 4.4063
		2.0826	2.30432	1.7179	1.64360	O2: 4.2758
		2.0494	2.35862	1.6933	1.64503	O3: 4.3626
		2.0494	2.35862	1.7372	1.66772	
		2.0304	2.32693	1.7276	1.66736	
		2.0309	2.32429	1.6871	1.65621	
		2.0363	2.30348			
		1.9855	2.32768			
		2.0048	2.31078			
		1.5979	2.42764			
	4O	2.1604	2.33661	1.8891	1.63356	O1: 4.2751
		2.0939	2.32015	1.9768	1.61832	O2: 4.1492
		2.0371	2.34213	1.8987	1.64051	O3: 4.3613
		2.0210	2.31449	1.8329	1.66554	O4: 4.1261
		2.0529	2.36183	1.7697	1.64925	
		2.0454	2.35171	1.7404	1.65316	
		2.0487	2.34450	1.6899	1.67462	
		2.0529	2.32527	1.6799	1.67034	
		2.0686	2.32756			
		2.0095	2.32386			
		1.6214	2.41121			

Table XXIV. Bond charge(BC), bond length (BL) and lone pair(LP) data for Si-Si and Si-O bonds for the inclusion of n numbers of O atoms (n=1,2,3 & 4) in Si-GB with vacancy V2.

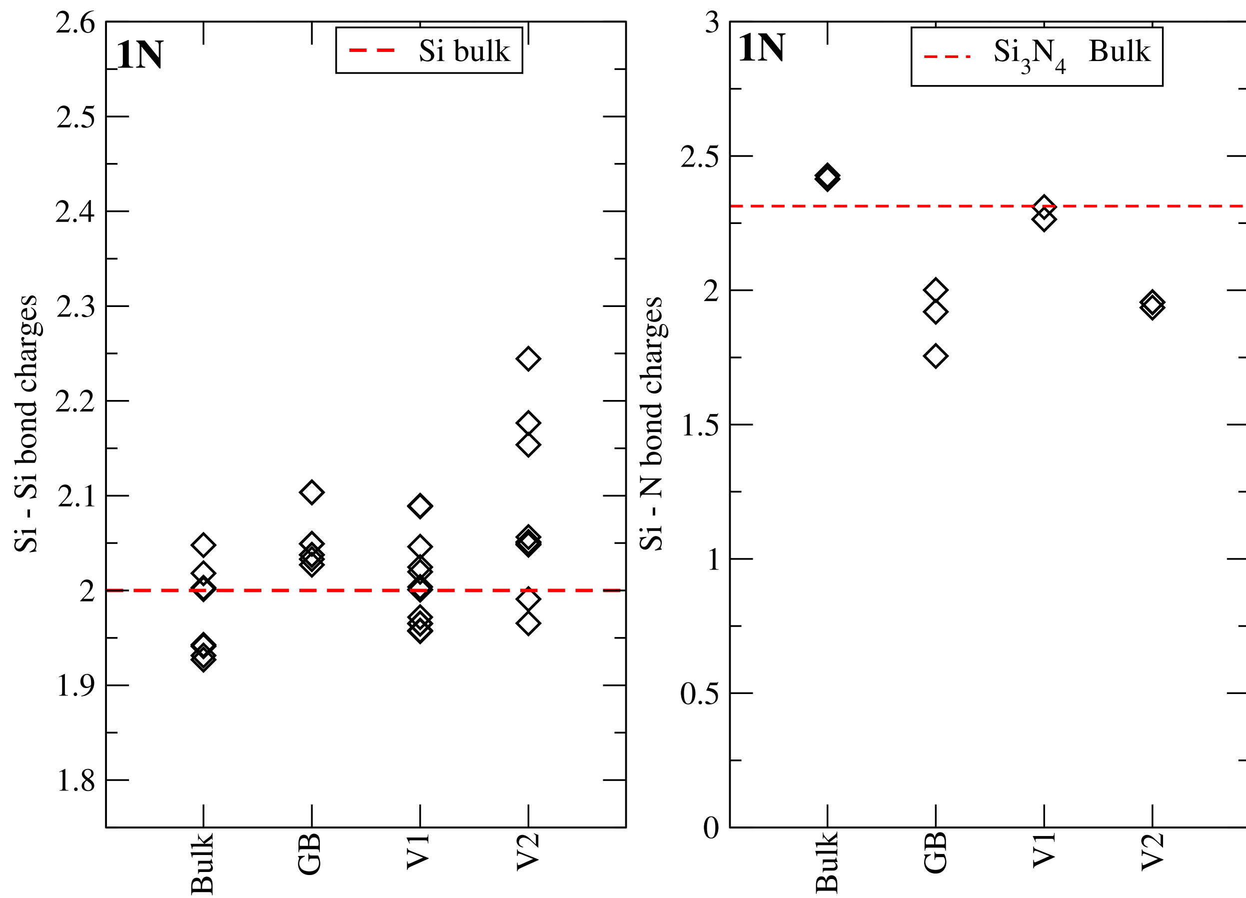

Figure 18. Bond charge variation of Si-Si and Si-N with the inclusion of one nitrogen atom in Si-bulk, Si-GB and in presence of vacancy V1 and V2. As a reference, Si-Si/Si-N bond charges from bulk phases of Si and Si_3N_4 are marked in the inset of respective plots.

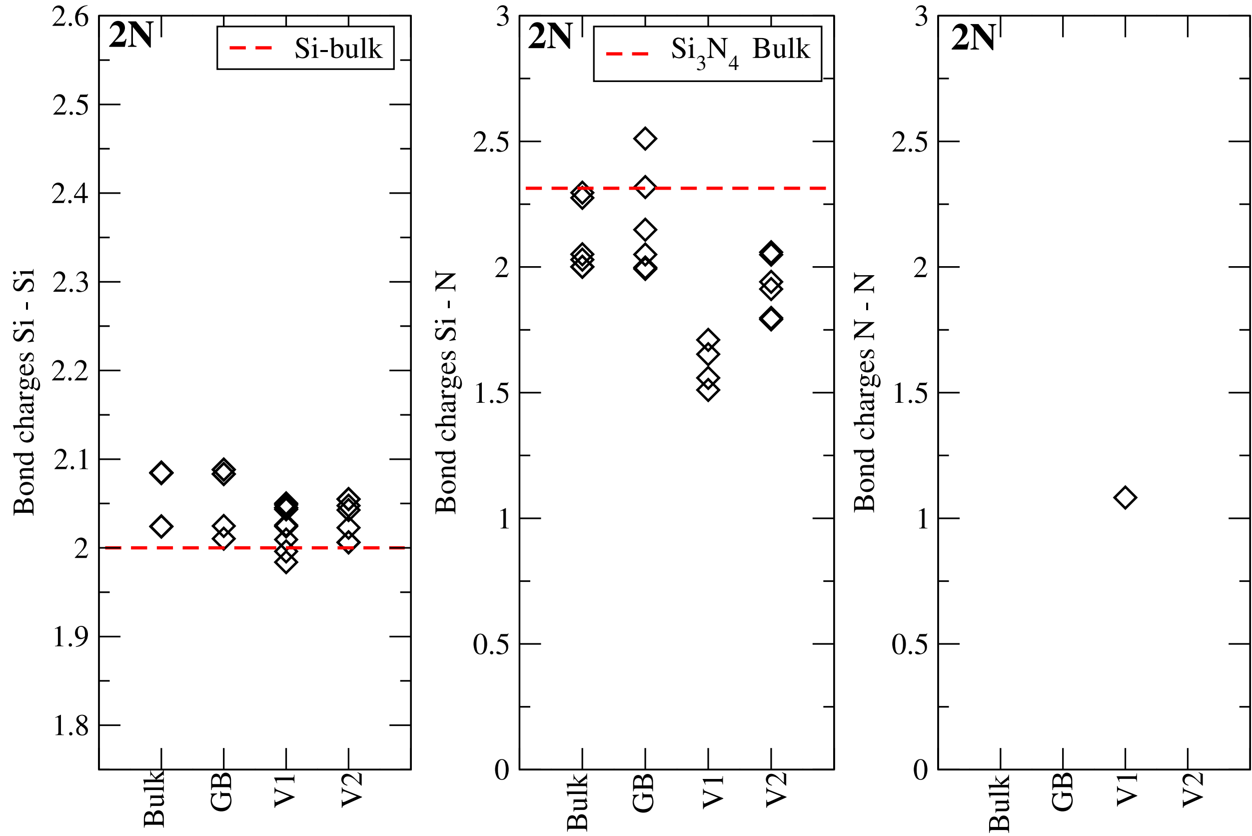

Figure 19. Bond charge variation of Si-Si, Si-N and N-N for the inclusion of two nitrogen atoms in Si-bulk, Si-GB and in presence of vacancy V1 and V2. As a reference, Si-Si/Si-N bond charges from bulk phases of Si and Si_3N_4 are marked in the inset of respective plots.

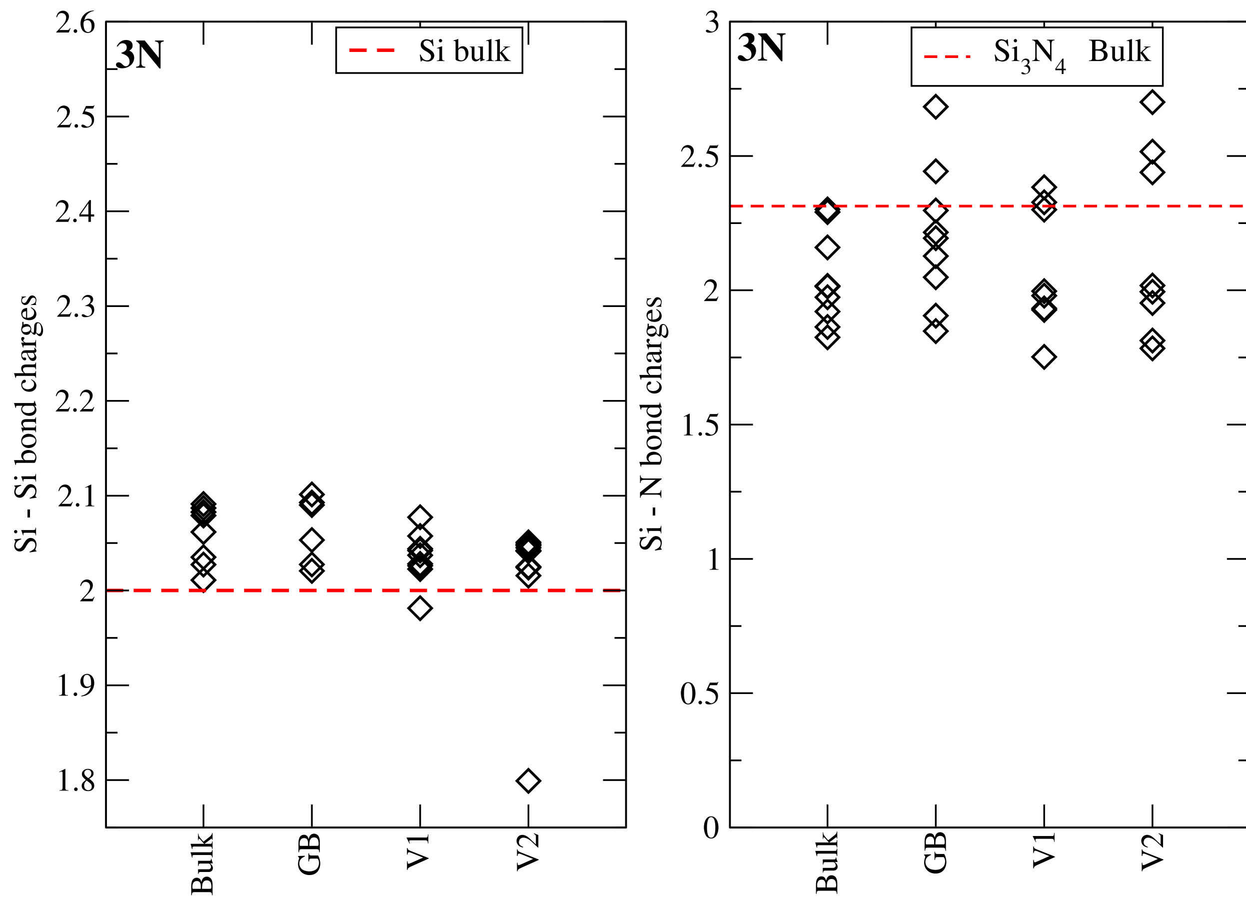

Figure 20. Bond charge variation of Si-Si and Si-N for the inclusion of three nitrogen atoms in Si-bulk, Si-GB and in presence of vacancy V1 and V2. As a reference, Si-Si/Si-N bond charges from bulk phases of Si and Si_3N_4 are marked in the inset of respective plots.

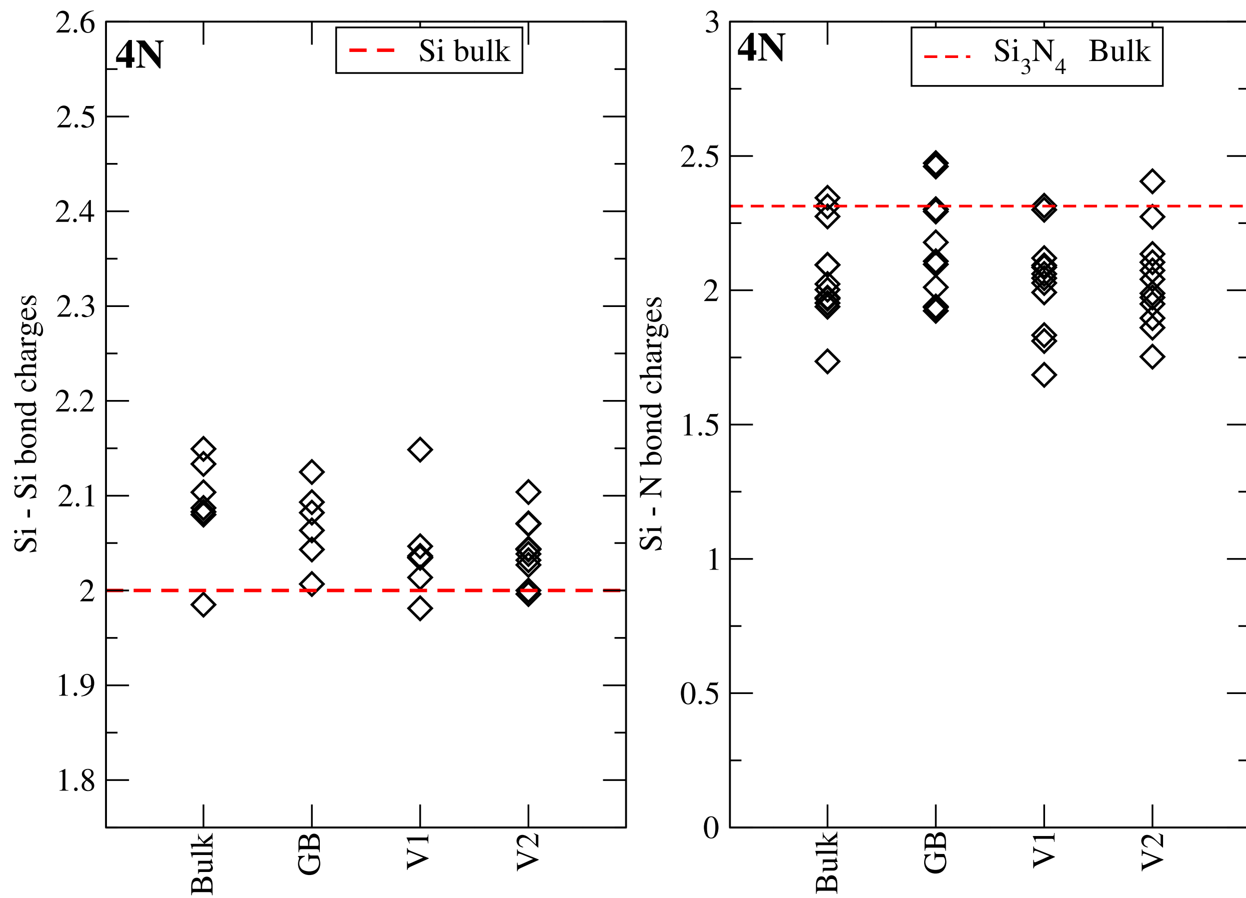

Figure 21. Bond charge variation of Si-Si and Si-N for the inclusion of four nitrogen atoms in Si-bulk, Si-GB and in presence of vacancy V1 and V2. As a reference, Si-Si/Si-N bond charges from bulk phases of Si and Si_3N_4 are marked in the inset of respective plots.

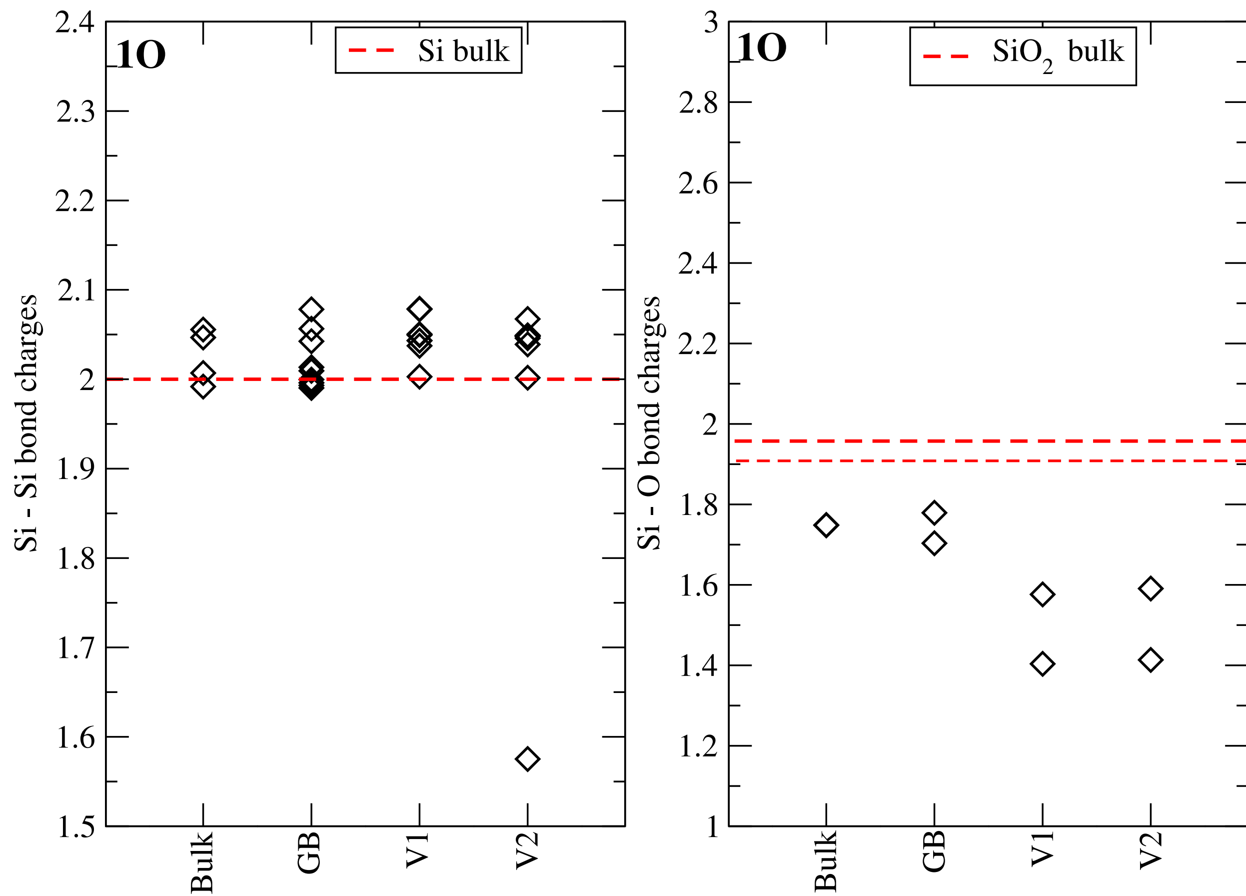

Figure 22. Bond charge variation of Si-Si and Si-O for the inclusion of one oxygen atom in Si-bulk, Si-GB and in presence of vacancy V1 and V2. As a reference, Si-Si/Si-O bond charges from bulk phases of Si and SiO_2 are marked in the inset of respective plots.

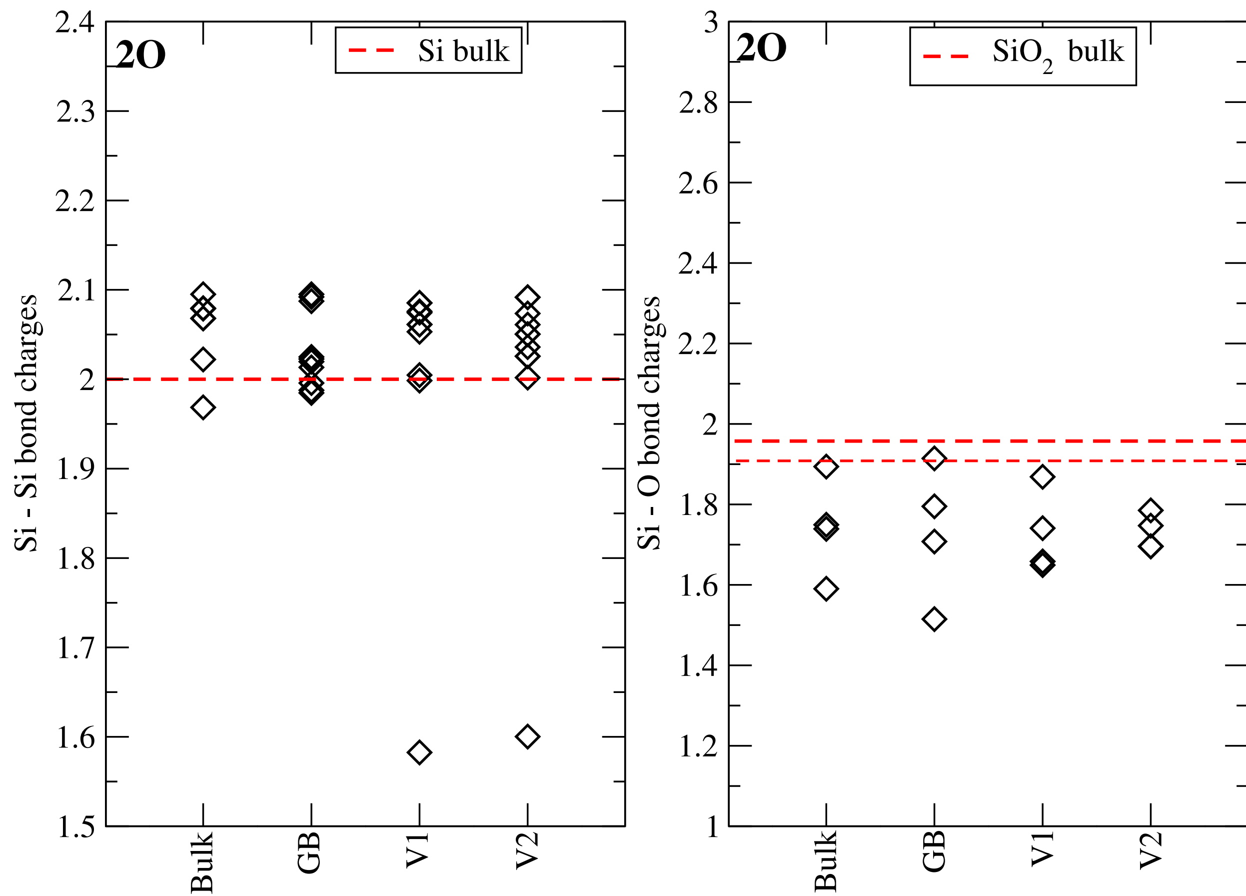

Figure 23. Bond charge variation of Si-Si and Si-O for the inclusion of two oxygen atoms in Si-bulk, Si-GB and in presence of vacancy V1 and V2. As a reference, Si-Si/Si-O bond charges from bulk phases of Si and SiO_2 are marked in the inset of respective plots.

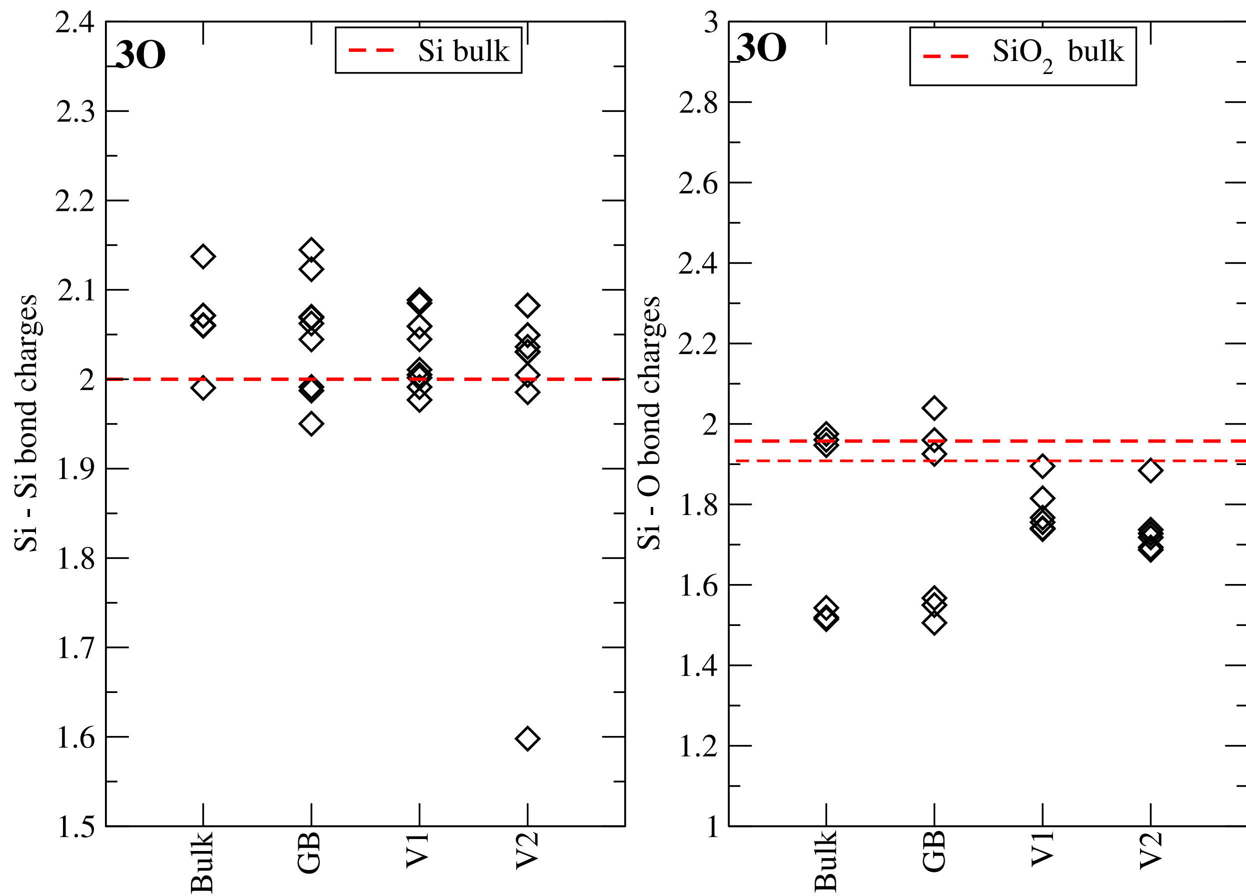

Figure 24. Bond charge variation of Si-Si and Si-O for the inclusion of three oxygen atoms in Si-bulk, Si-GB and in presence of vacancy V1 and V2. As a reference, Si-Si/Si-O bond charges from bulk phases of Si and SiO_2 are marked in the inset of respective plots.

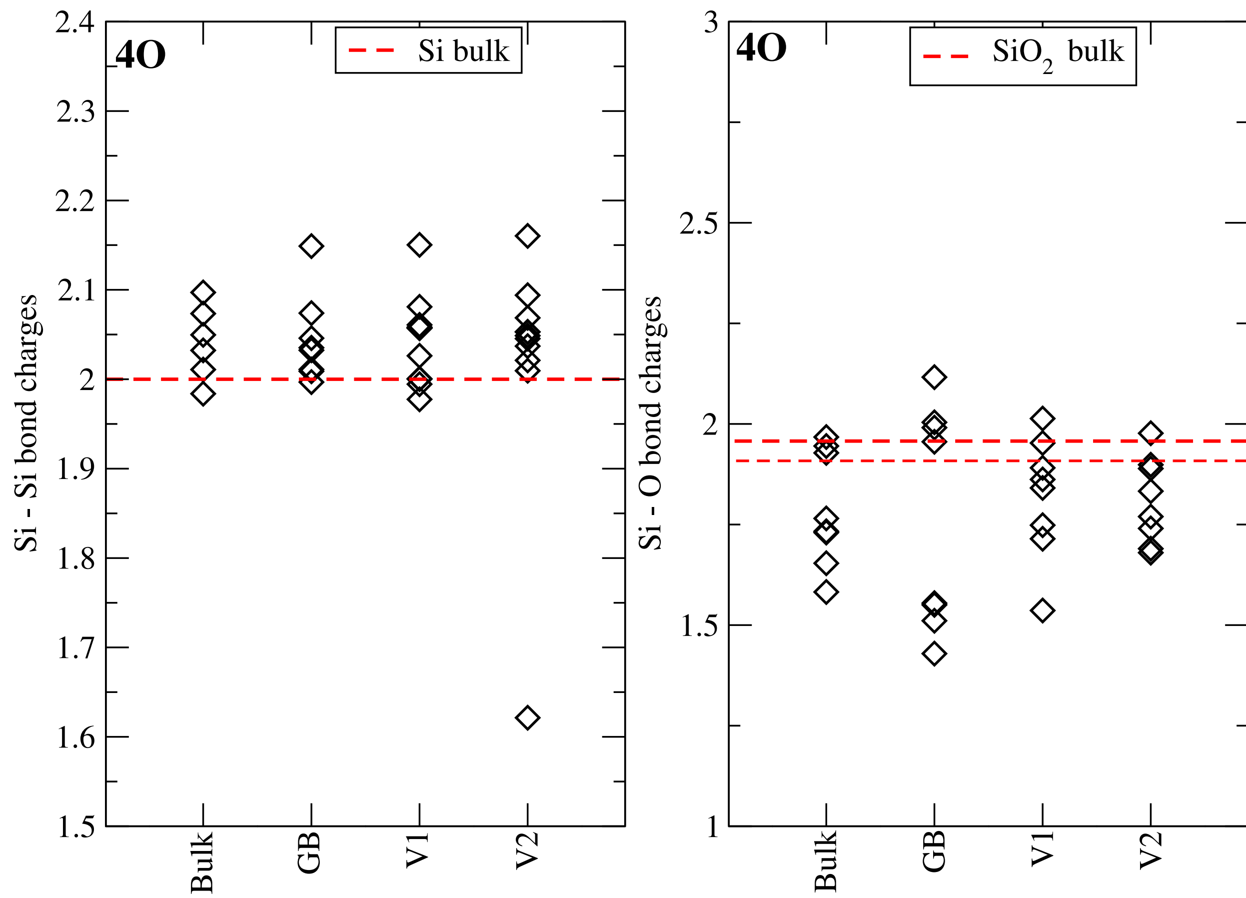

Figure 25. Bond charge variation of Si-Si and Si-O for the inclusion of four oxygen atoms in Si-bulk, Si-GB and in presence of vacancy V1 and V2. As a reference, Si-Si/Si-O bond charges from bulk phases of Si and SiO_2 are marked in the inset of respective plots.

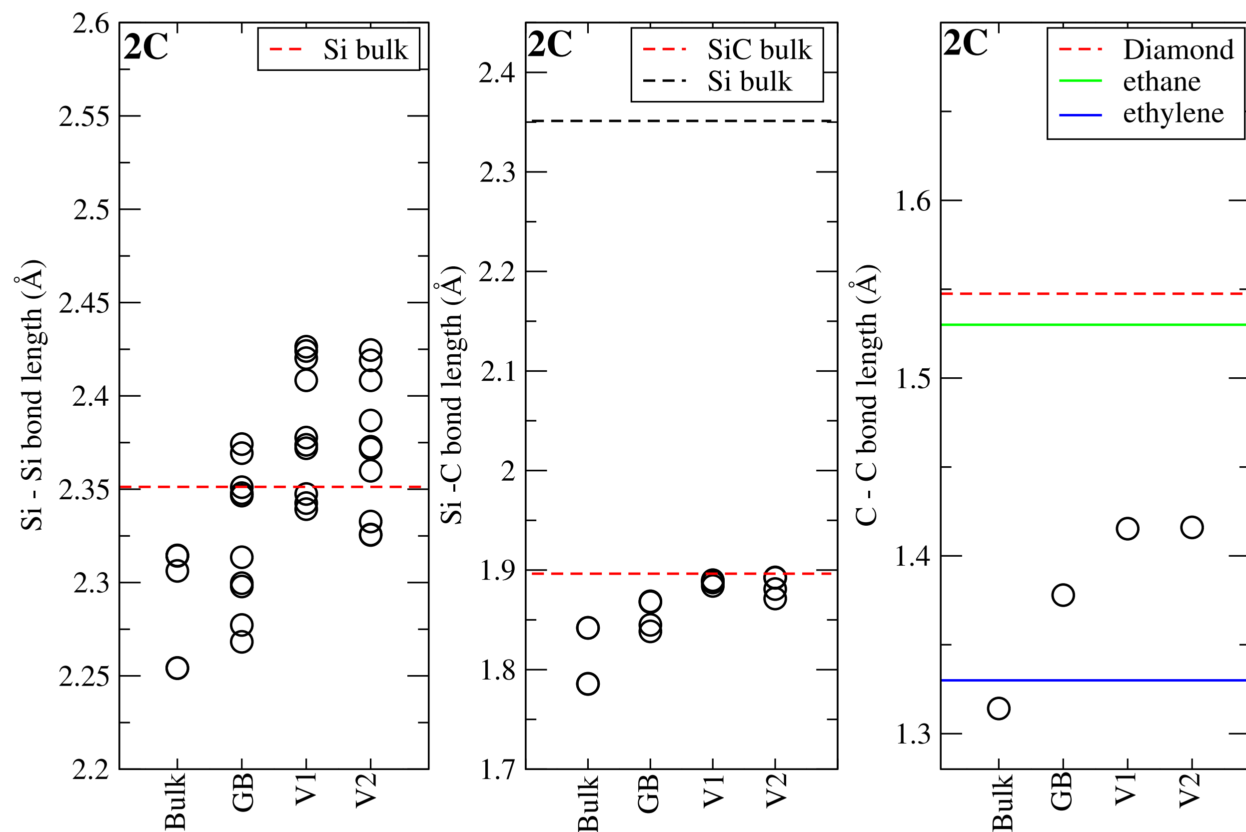

Figure 26. Bond length variation of Si-Si, Si-C and C-C for the inclusion of two carbon atoms in Si-bulk, Si-GB and in presence of vacancy V1 and V2. As a reference, Si-Si/Si-C/C-C bond length from bulk phases of Si, SiC, diamond and molecular systems ethylene and ethane are marked in the inset of respective plots.

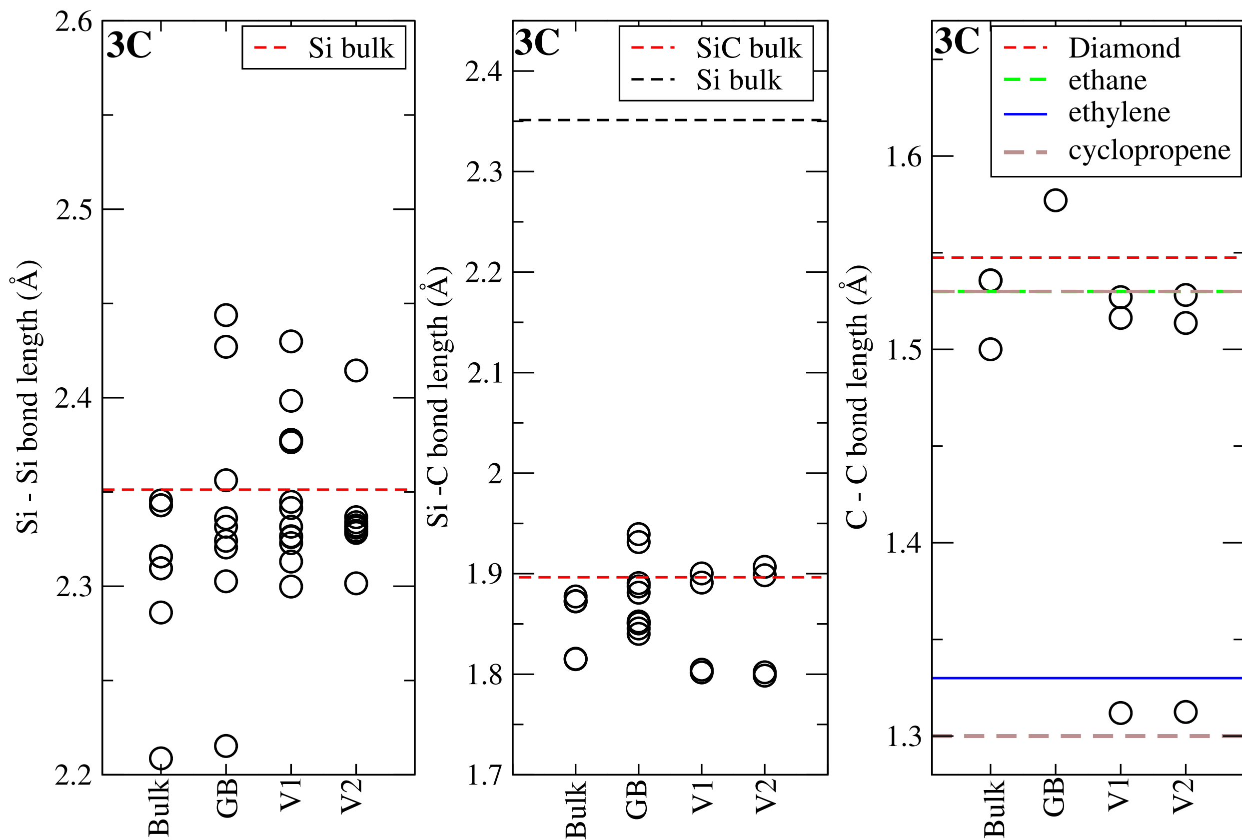

Figure 27. Bond length variation of Si-Si, Si-C and C-C for the inclusion of three carbon atoms in Si-bulk, Si-GB and in presence of vacancy V1 and V2. As a reference, Si-Si/Si-C/C-C bond length from bulk phases of Si, SiC, diamond and molecular systems ethylene, ethane, and cyclopropen are marked in the inset of respective plots

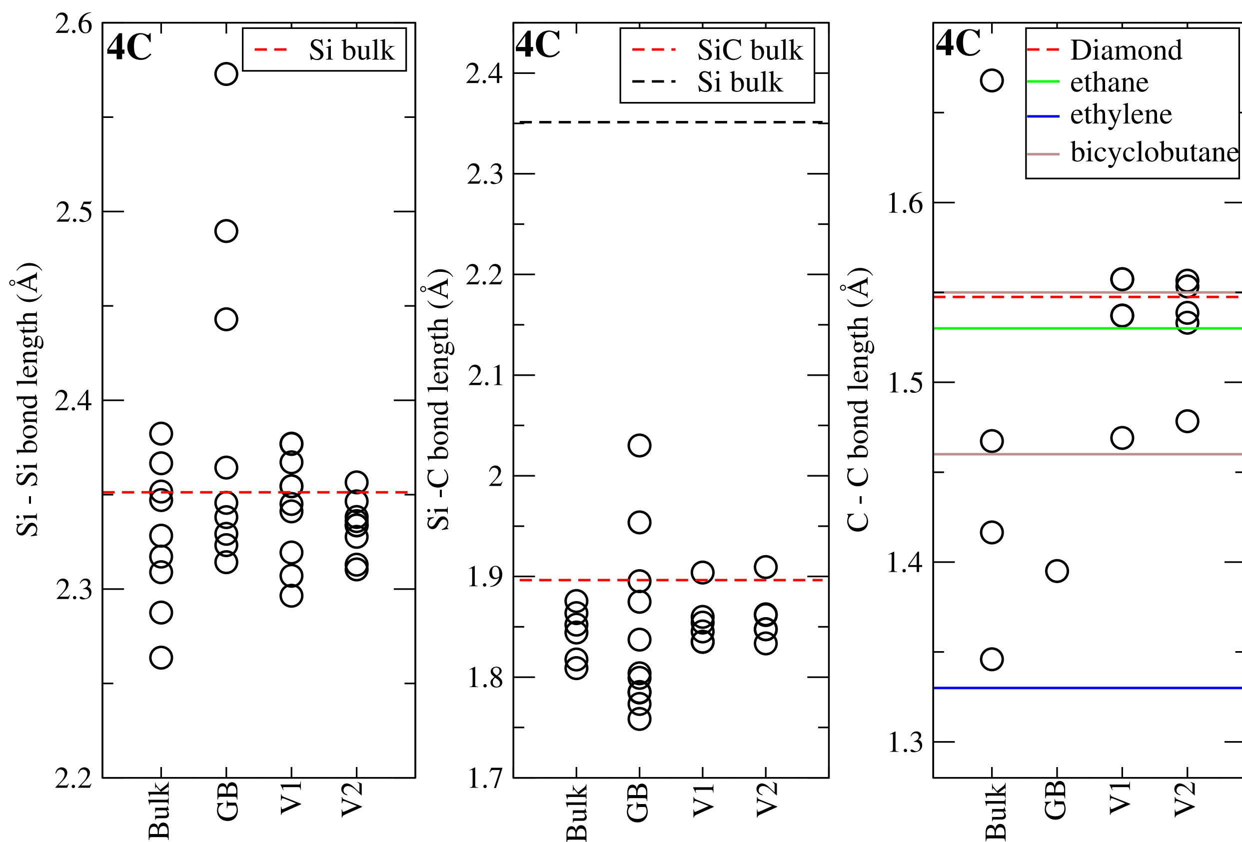

Figure 28. Bond length variation of Si-Si, Si-C and C-C for the inclusion of four carbon atoms in Si-bulk, Si-GB and in presence of vacancy V1 and V2. As a reference, Si-Si/Si-C/C-C bond length from bulk phases of Si, SiC, diamond and molecular systems ethylene, ethane, and bicyclobutane are marked in the inset of respective plots

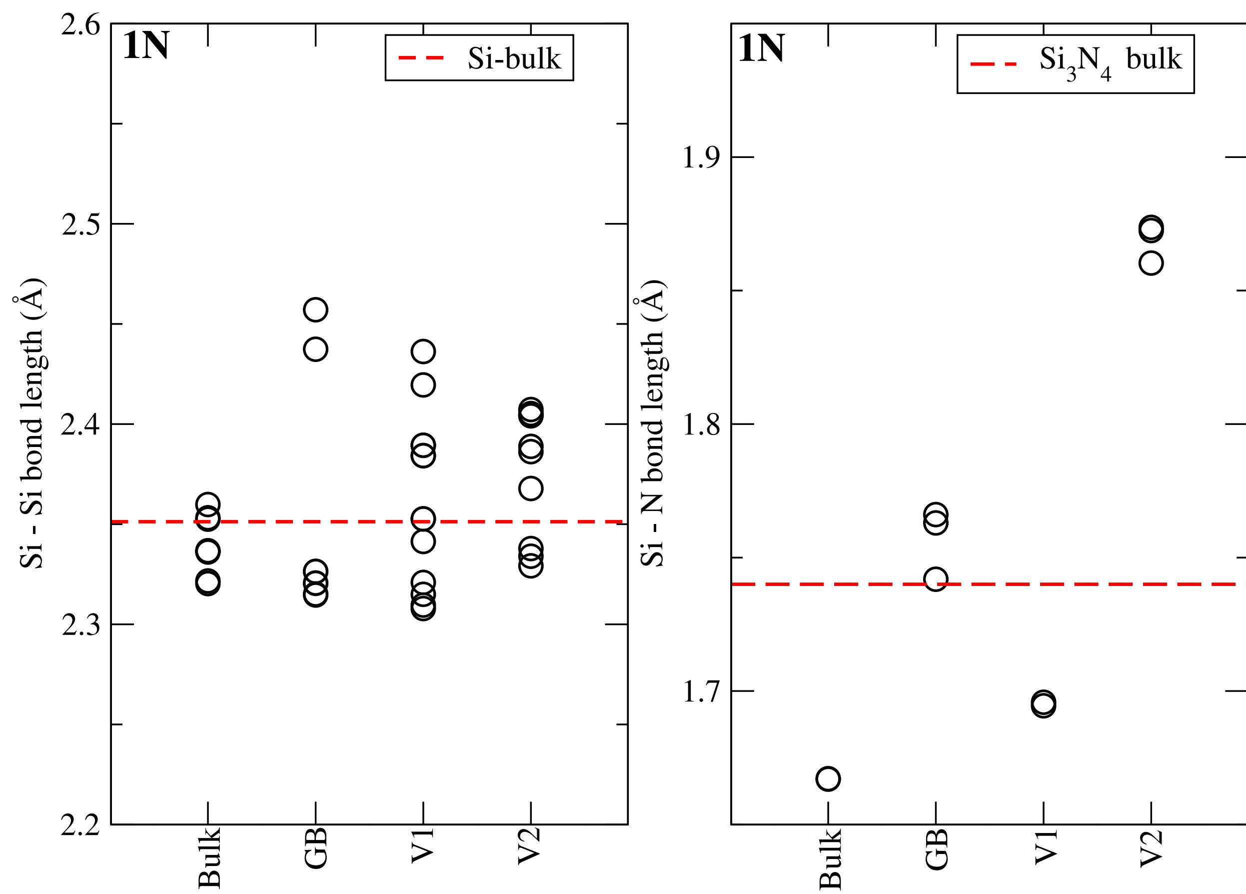

Figure 29. Bond length variation of Si-Si and Si-N for the inclusion of one nitrogen atom in Si-bulk, Si-GB and in presence of vacancy V1 and V2. As a reference, Si-Si/Si-N bond length from bulk phases of Si, Si_3N_4 are marked in the inset of respective plots.

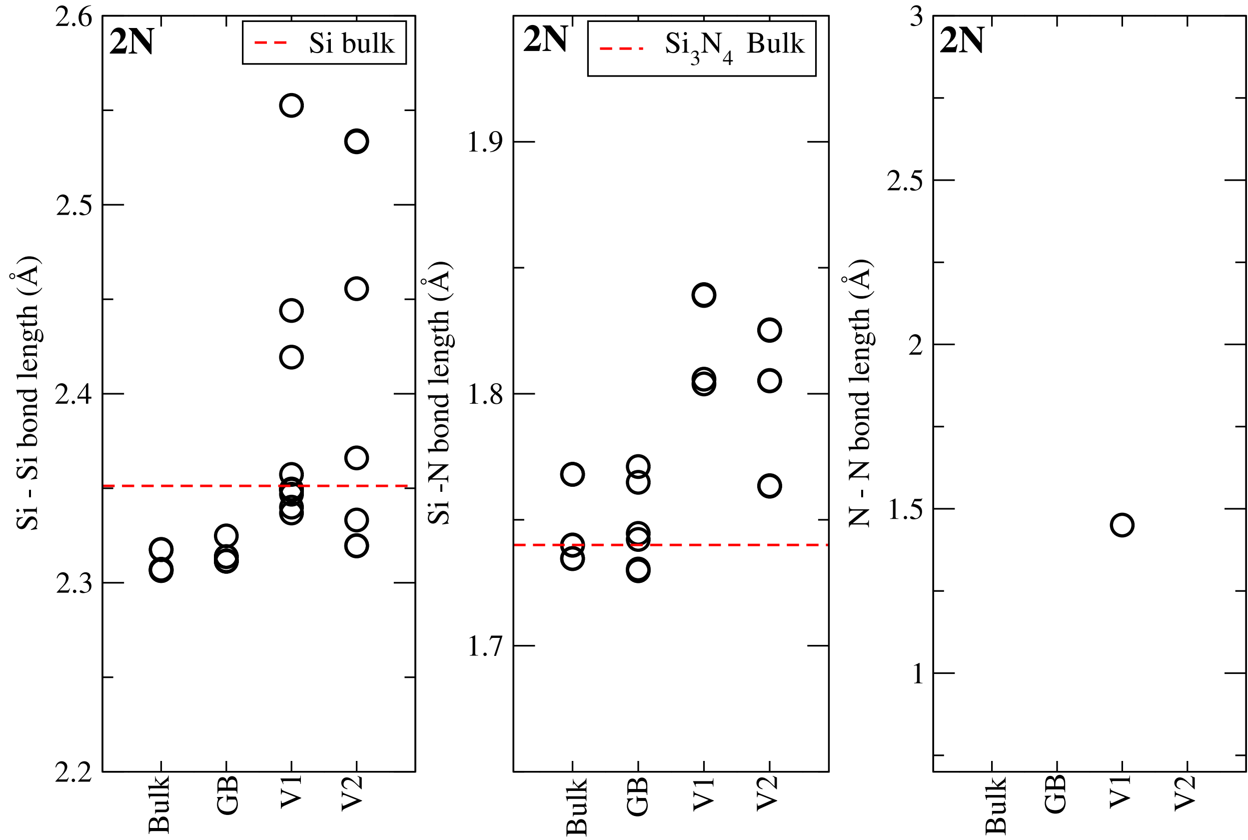

Figure 30. Bond length variation of Si-Si, Si-N and N-N for the inclusion of two nitrogen atoms in Si-bulk, Si-GB and in presence of vacancy V1 and V2. As a reference, Si-Si/Si-N bond length from bulk phases of Si, Si_3N_4 are marked in the inset of respective plots.

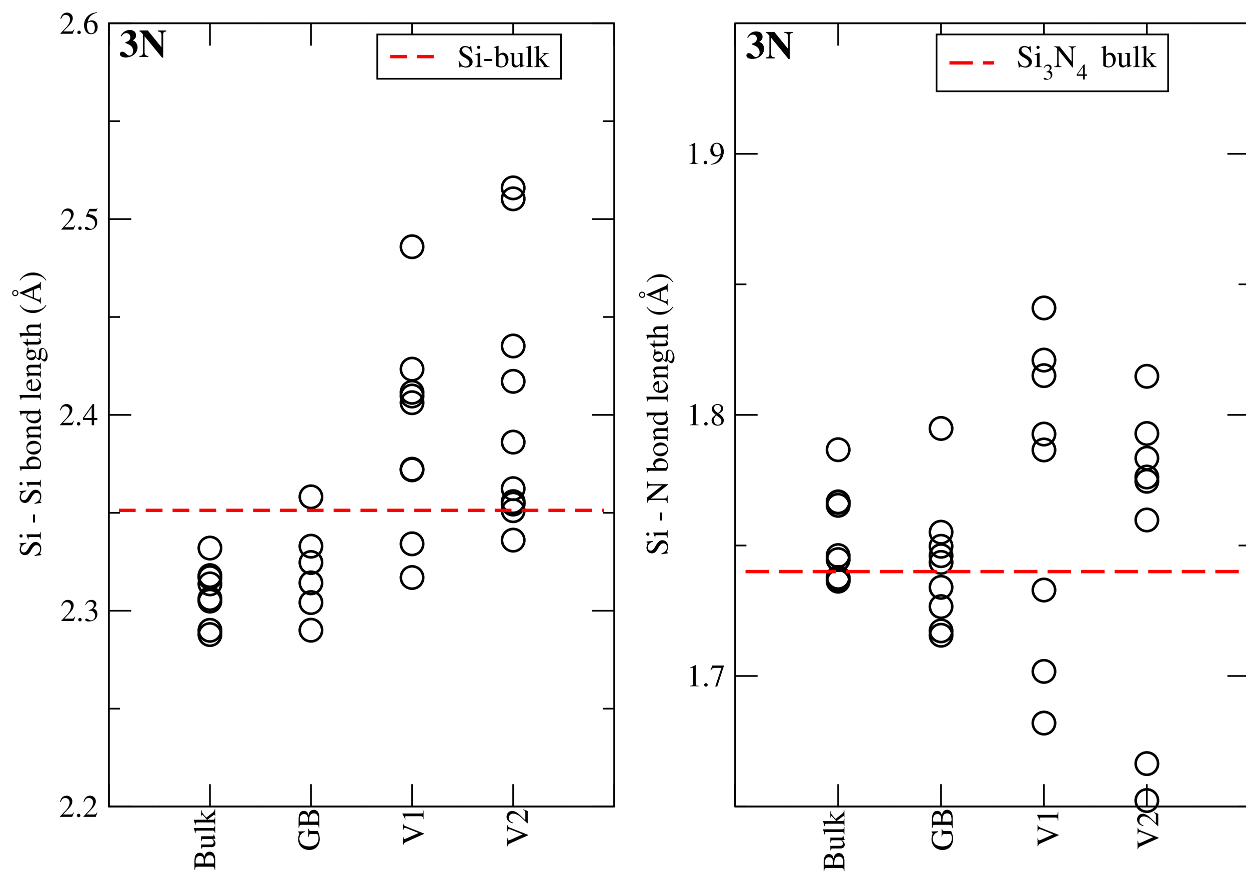

Figure 31. Bond length variation of Si-Si and Si-N for the inclusion of three nitrogen atom in Si-bulk, Si-GB and in presence of vacancy V1 and V2. As a reference, Si-Si/Si-N bond length from bulk phases of Si, Si_3N_4 are marked in the inset of respective plots.

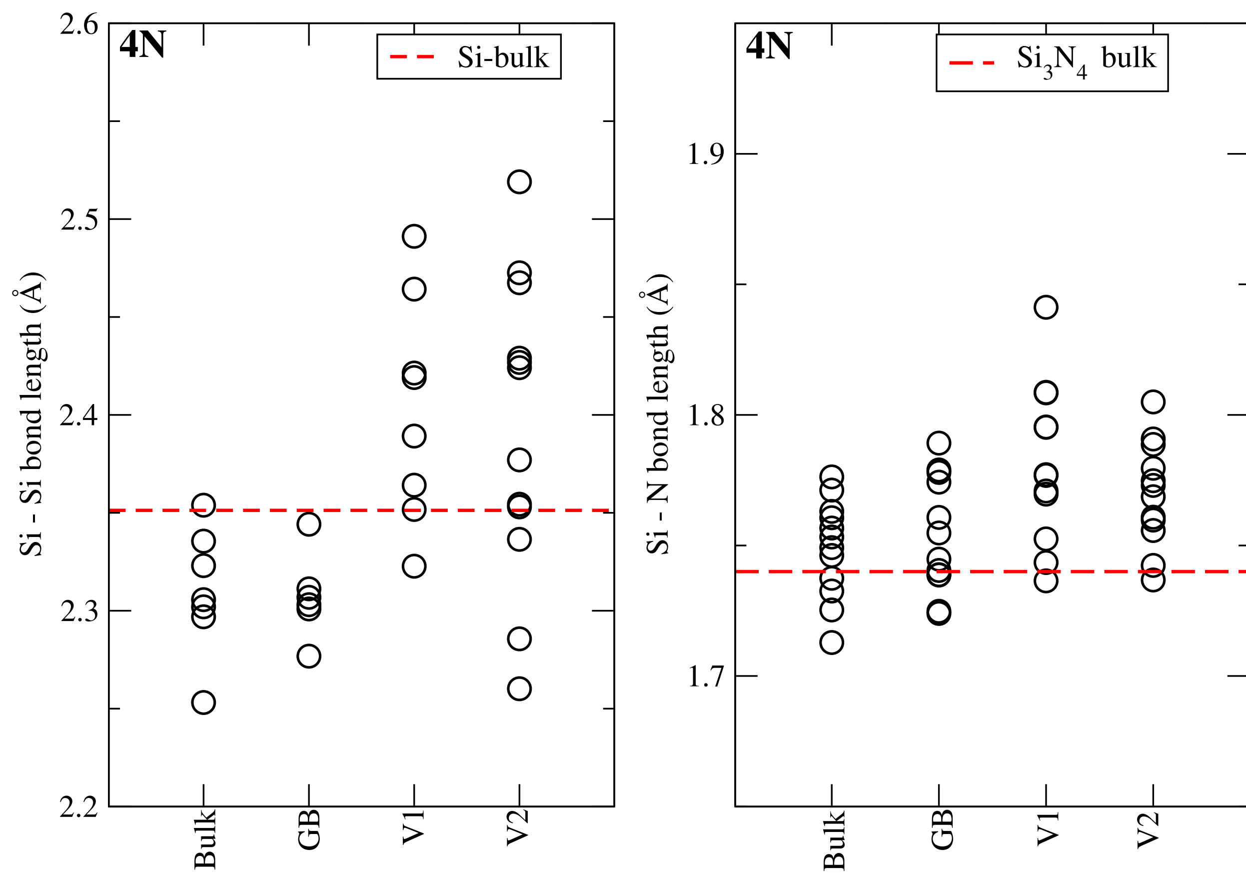

Figure 32. Bond length variation of Si-Si and Si-N for the inclusion of four nitrogen atom in Si-bulk, Si-GB and in presence of vacancy V1 and V2. As a reference, Si-Si/Si-N bond length from bulk phases of Si, Si_3N_4 are marked in the inset of respective plots.

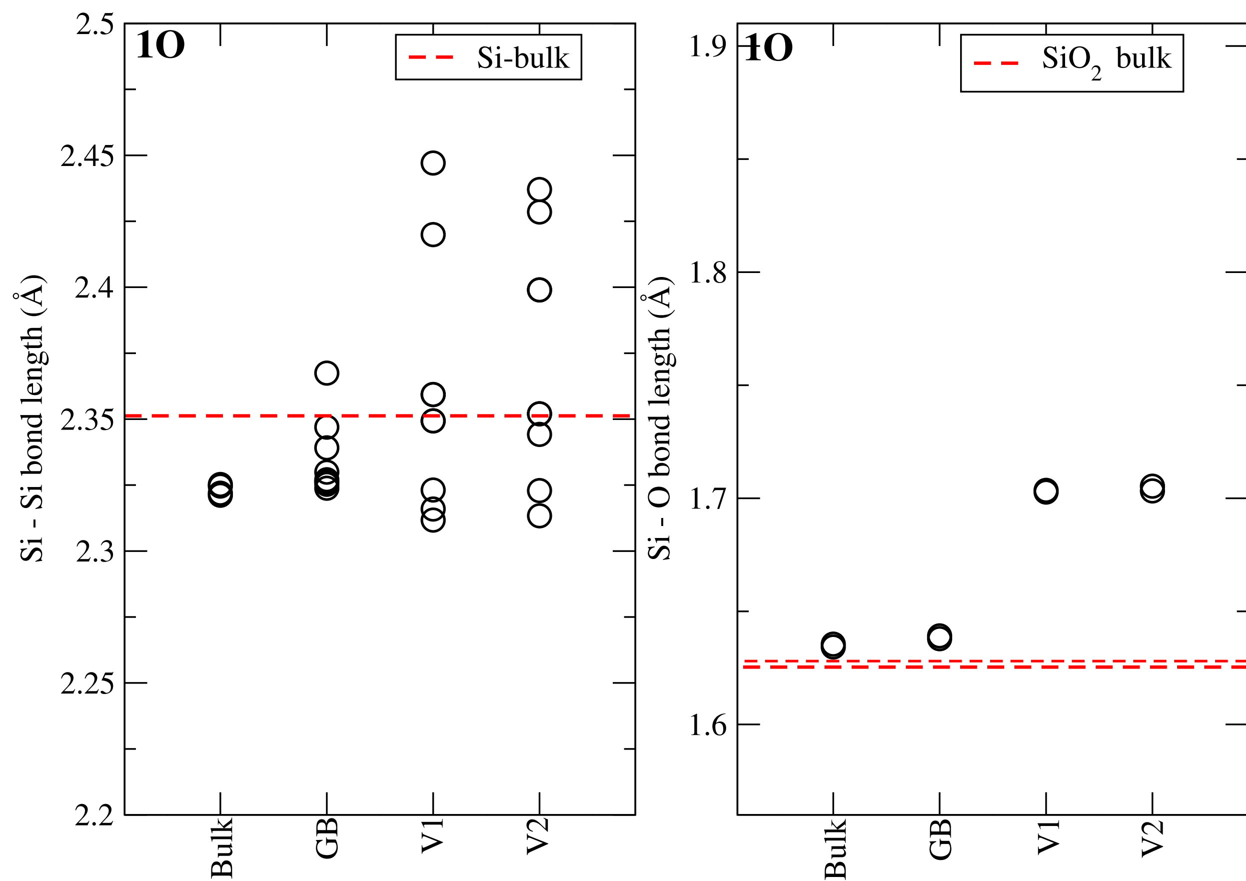

Figure 33. Bond length variation of Si-Si and Si-O for the inclusion of one oxygen atom in Si-bulk, Si-GB and in presence of vacancy V1 and V2. As a reference, Si-Si/Si-O bond length from bulk phases of Si, SiO_2 are marked in the inset of respective plots.

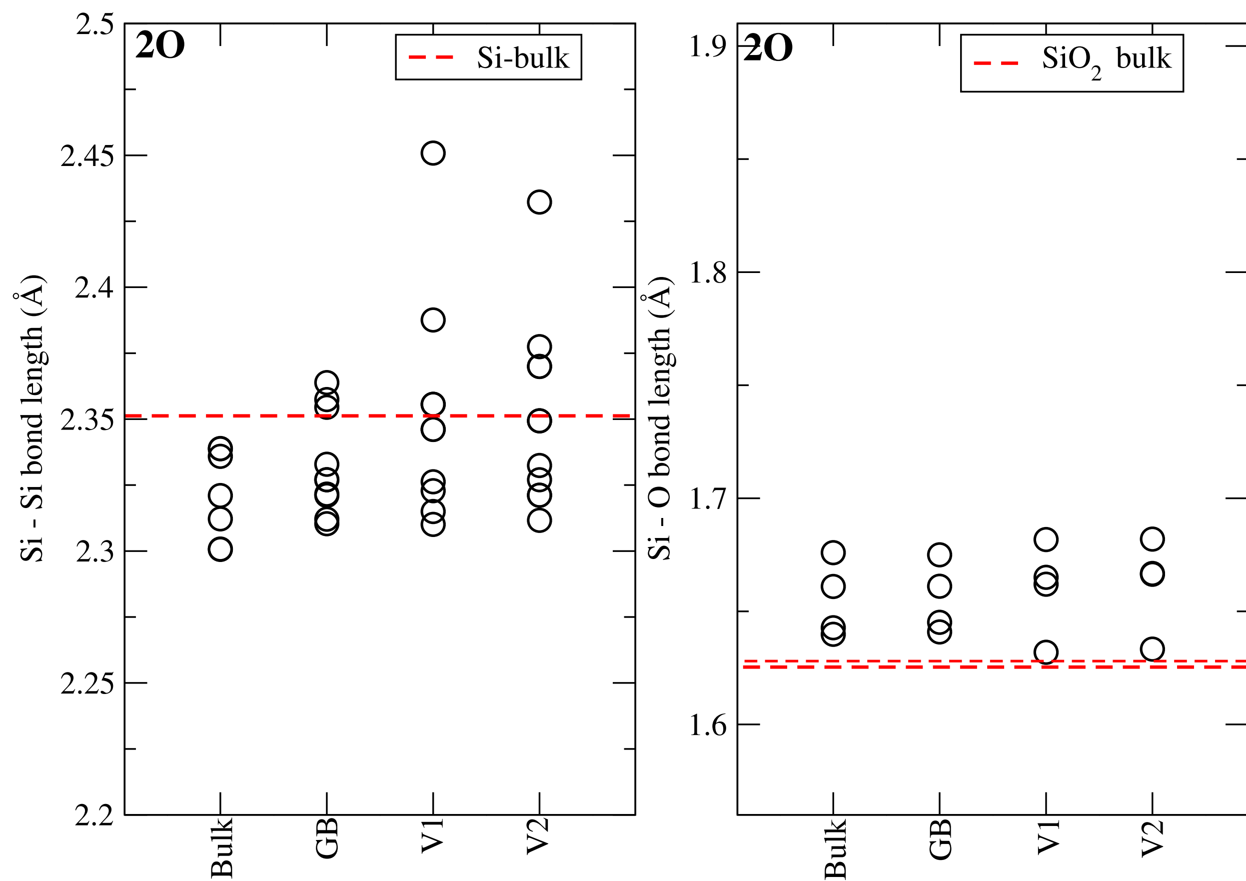

Figure 34. Bond length variation of Si-Si and Si-O for the inclusion of two oxygen atoms in Si-bulk, Si-GB and in presence of vacancy V1 and V2. As a reference, Si-Si/Si-O bond length from bulk phases of Si, SiO_2 are marked in the inset of respective plots.

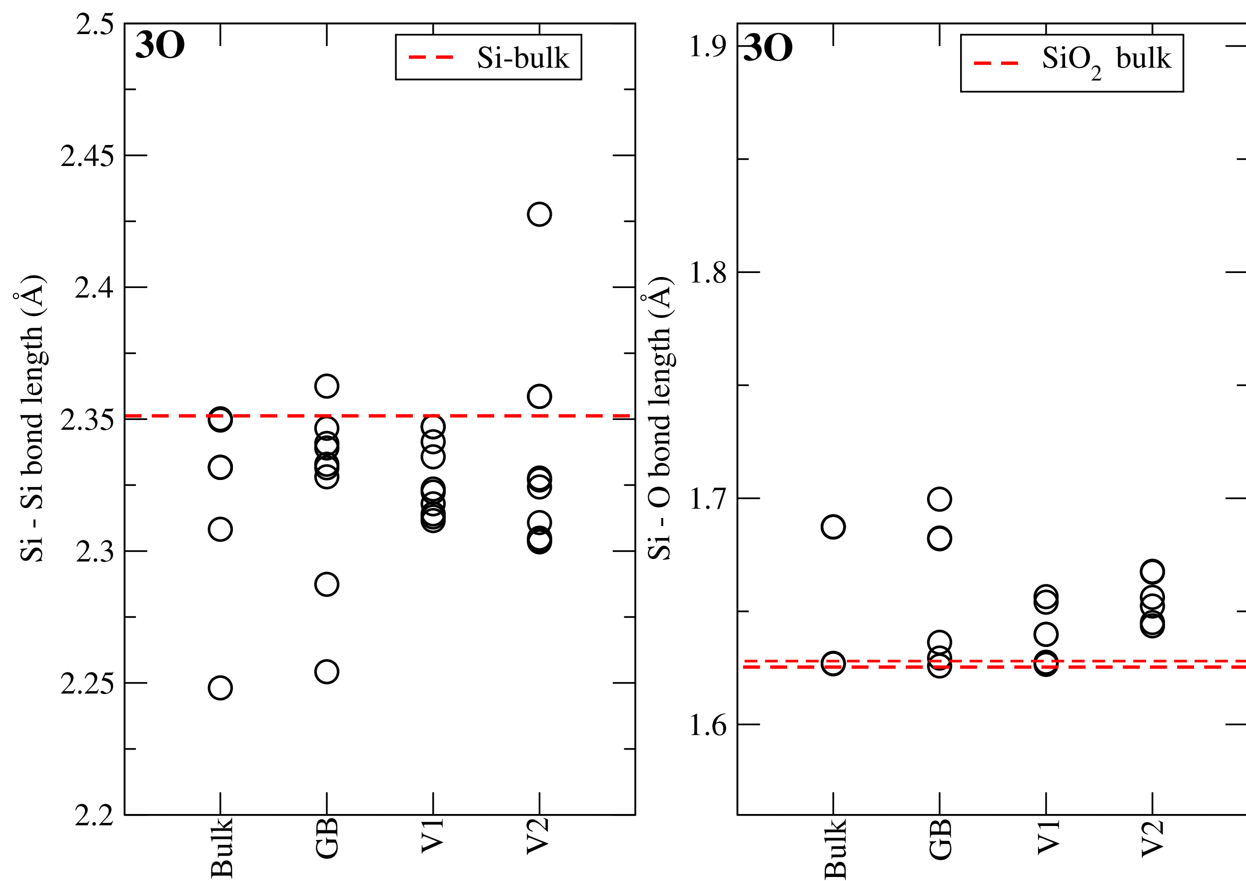

Figure 35. Bond length variation of Si-Si and Si-O for the inclusion of three oxygen atoms in Si-bulk, Si-GB and in presence of vacancy V1 and V2. As a reference, Si-Si/Si-O bond length from bulk phases of Si, SiO_2 are marked in the inset of respective plots.

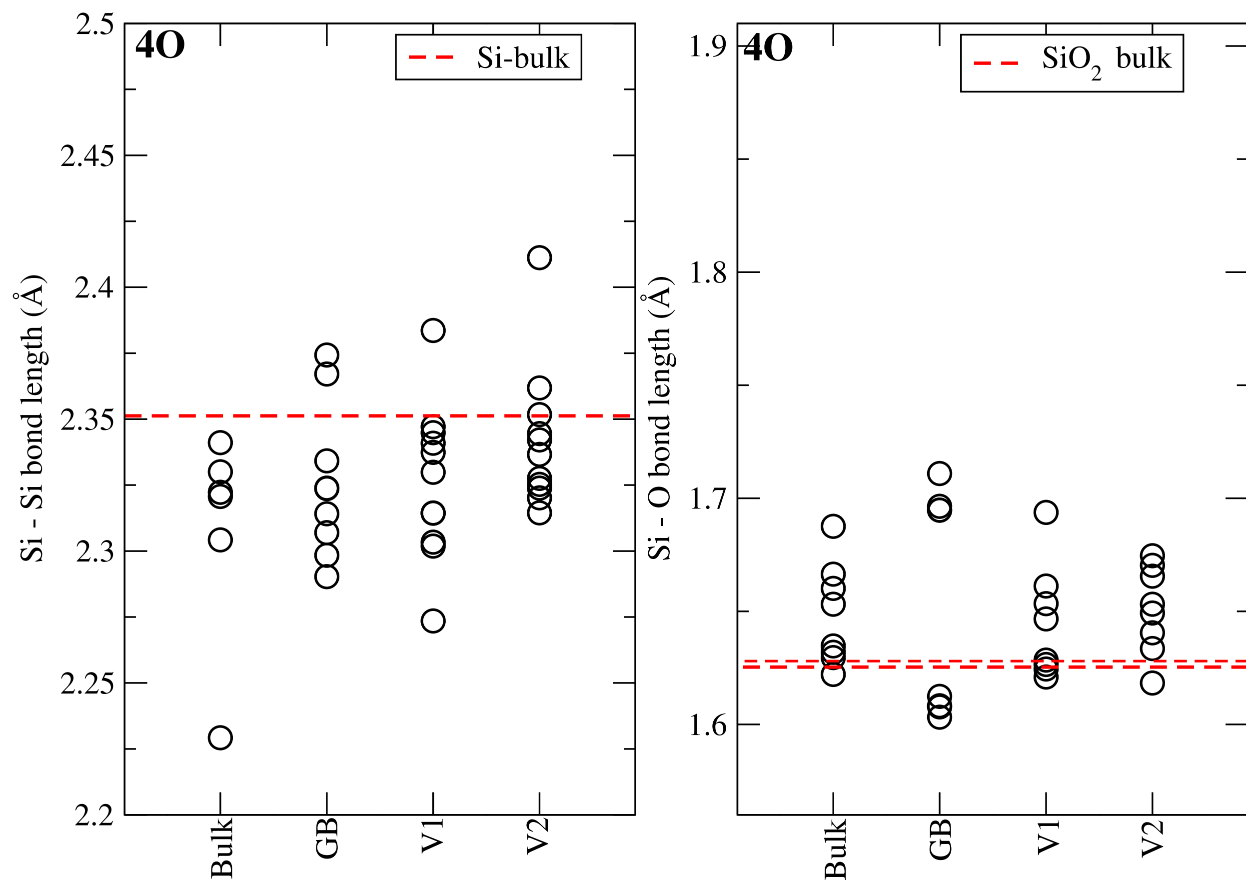

Figure 36. Bond length variation of Si-Si and Si-O for the inclusion of four oxygen atoms in Si-bulk, Si-GB and in presence of vacancy V1 and V2. As a reference, Si-Si/Si-O bond length from bulk phases of Si, SiO_2 are marked in the inset of respective plots.